Singularity induced exterior and interior Stokes flows

Prabir Daripa[a] and D. Palaniappan
Department of Mathematics, Texas A&M University, College Station, Texas 77843

(Received 18 July 2000; accepted 31 July 2001)

In this paper, the two-dimensional Stokes flow inside and outside a circular cylinder induced by a pair of line singularities (rotlet and stokeslet) is studied. Analytical solutions for the flow field are obtained by straightforward application of the Fourier method. The streamline patterns are sketched for a number of special cases where the cylinder is either stationary or rotating about its own axis. In particular, some interesting flow patterns are observed in the parameter space which may have potential significance in studies of various flows including flows in journal bearing, mixing flows, chaotic flows, etc. We also investigate into the way the streamline topologies change as the parameters are varied. © *2001 American Institute of Physics.* [DOI: 10.1063/1.1407269]

I. INTRODUCTION

The solutions of problems involving application of point forces and torques are of considerable interest in continuum mechanics. These solutions can be used in the representation of solutions of more complicated and physically realizable problems. The fundamental solution for a point force (i.e., a free-space Green's function for the biharmonic equation) in an incompressible homogeneous unbounded slow viscous flow is called a ''stokeslet'' and can be extracted from the Stokes solution for the flow past a sphere[1] (see also Refs. 2–5). Another primary singularity in the theory of viscous hydrodynamics is the ''rotlet'' or ''couplet'' (see Ref. 6). The singularities of slow viscous flow have been known from the works of Lorentz,[7] Oseen,[8] and Burgers.[9] Some elegant application of these singularities in three-dimensional boundary value problems may be found in the works of Batchelor,[6] Blake,[10] Blake and Chwang,[11] among many others.

In the case of two-dimensional creeping flows, a study of singularity solutions has been the topic of many researchers. One of the interesting and unusual phenomena associated with the plane Stokes flow is the Stokes paradox which is a consequence of the fact that there is no solution to the biharmonic equation that represents slow streaming flow past a finite body. The cause and resolution of this paradox was explained by Kaplun and Lagerstrom[12] and Proudman and Pearson.[13] However, Jeffery[14] showed that two cylinders of equal radius rotating with equal but opposite angular velocities produce a uniform flow at large distances. Jeffery's work was the catalyst for many investigations concerning locally generated two-dimensional Stokes flows. Dorrepaal *et al.*[15] found a uniform stream in situations when a rotlet or a stokeslet is located in front of a circular cylinder. The rotlet model has also been used in the stirring mechanism inside a corrugated boundary.[16] The potential flow singularities such as a source, a sink, a doublet, etc., when placed in front of a cylinder also produce a uniform flow at large distances as shown by Smith[17] and Avudainayagam *et al.*[18] Furthermore, the image solutions for a rotlet and stokeslet are also used in the interpretation of the results for two cylinders rotating in a viscous fluid.[19]

In the first part of this paper we study Stokes flows past a circular cylinder generated by a pair of rotlets and stokeslets. The corresponding problem for Stokes flow with potential source-sink combination in the presence of a circular as well as an elliptic cylinder was investigated by Smith.[17] In Ref. 17, the source and the sink were located equidistant from the cylinder. One of the main conclusions in Ref. 17 was that a uniform flow always exists for this combination. However, this fact is not true if the singularities either have unequal strengths or are located nonequidistant from the cylinder. We illustrate this by choosing rotlets and stokeslets of different strengths in the present study. In particular, we show that the rotlets-cylinder combination produces interesting flow patterns in the presence of cylinder rotation. In the case of a stokeslets-cylinder combination, the flow structure is also modified considerably. These interesting features of the flow fields do not seem to have been noticed before.

In the second part of the paper we investigate the flows inside a cylinder generated by a pair of rotlets and stokeslets. These bounded viscous flows abound in nature as well as in many areas of practical interest such as journal bearing, stirring, and mixing of viscous fluids, etc. An insight into various mechanisms and flow topologies of such flows with respect to available free parameters can be beneficial to improving the performance of various systems involving such flows. To gain such insight, it is usually desirable to design models that retain the basic flow features of the complex problem, yet simple enough to be analyzed accurately using a combination of analysis and numerics. In this connection, it is worth mentioning that the most common model that has been used to demonstrate stirring process is the two-dimensional Stokes flows generated by singularities inside a circular cylinder. In these models, a line rotlet, which may be regarded as a rotating cylinder of infinitesimal radius, has been used as a model for a stirrer. Incidentally, this flow is topologically equivalent to the flow between two eccentric

[a]Author to whom correspondence should be addressed; electronic mail: prabir.daripa@math.tamu.edu

circular cylinders with inner or both cylinders rotating, which models flow in a journal bearing (see Ref. 20 for a comprehensive analysis of journal bearing flow). It is worth citing the work of Jana *et al.*,[21] who have recently attempted to explain vortex mixing flows using two finite cylinders rotating slowly in a cylindrical volume of viscous fluid. There are many studies of mixing and other interior Stokes flows which are not cited here but can be found in the literature.

The paper is organized as follows. In Sec. II, we formulate the problem of Stokes flow in two-dimensions in terms of stream function. The solutions for exterior flow problems are presented in Sec. III. First, we provide the solution for a pair of rotlets in the presence of a circular cylinder in Sec. III A. The solution is presented in singularity form with the interpretation of image singularities. The far-field behavior is discussed briefly, followed by the derivation of the limiting case for a two-dimensional plane boundary. The interesting features of the flow fields including existence of eddies are also discussed there. Similar calculations and discussions are repeated for a pair of stokeslets with their axes along the *x*-direction in Sec. III B. The striking features of the flow fields in this case are also presented in this subsection. The singularity solution for a pair of stokeslets with their axes along *y*-direction is provided in Sec. III C. Here again, the far-field behavior, the limiting case, and the flow structure are discussed in detail. Section IV contains the discussion of interior Stokes flows generated by a pair of rotlets and a pair of stokeslets (with their axes along either the *x* or *y* direction). The streamline topologies are discussed in each case in the respective subsections. Finally, main results of the paper are summarized in Sec. V.

II. MATHEMATICAL PRELIMINARIES

We consider the slow steady flow (also known as creeping flow/Stokes flow) of a viscous incompressible fluid past an infinite circular rigid cylinder of radius a. The governing equations are the linearized steady Navier–Stokes equations (also known as Stokes equations) given by

$$\mu \nabla^2 \mathbf{u} = \nabla p, \tag{1}$$

$$\nabla \cdot \mathbf{u} = 0. \tag{2}$$

Here $\mathbf{u}$ is the two-dimensional velocity vector with components (u_r, u_θ) in the radial and transverse directions (r, θ), respectively, p the pressure, and μ the coefficient of viscosity of the fluid. It is well-known that the Stokes equations (1) and (2) (in two-dimensions) when expressed in terms of stream function $\psi(r, \theta)$, reduce to

$$\nabla^4 \psi = 0, \tag{3}$$

where

$$\nabla^2 = \frac{\partial^2}{\partial r^2} + \frac{1}{r}\frac{\partial}{\partial r} + \frac{1}{r^2}\frac{\partial^2}{\partial \theta^2}.$$

The velocity components in r and θ directions are given by

$$u_r = -\frac{1}{r}\frac{\partial \psi}{\partial \theta}, \tag{4}$$

$$u_\theta = \frac{\partial \psi}{\partial r}. \tag{5}$$

We assume that the cylinder is impenetrable and there is no slip on the surface. In terms of stream function these boundary conditions become

$$\psi = \frac{\partial \psi}{\partial r} = 0, \quad \text{on} \quad r = a. \tag{6}$$

The far-field boundary condition could make the problem ill-posed in several situations. The simplest example of this kind is the ''Stokes paradox'' which illustrates that there is no solution to Eq. (3) subject to the boundary conditions Eq. (6) and a uniform flow at infinity. However, in the case of singularity driven flows, the ill-posedness disappears and one could obtain the solutions of the two-dimensional Stokes equations with finite velocities at large distances from the cylinder. In other words, the singularity driven Stokes flow problems in two-dimensions are well-posed. For singularity driven flows, one must also have

$$\psi \sim \psi_s, \quad \text{as} \quad R \to 0, \tag{7}$$

where ψ_s corresponds to the stream function only due to the singularity and R is the distance of the field point measured from the singularity.

We now proceed to present solutions for two-dimensional Stokes flows outside/inside a circular cylinder due to a pair of rotlets and stokeslets separately. The exact solutions have been used to depict the flow topologies for a number of cases where the cylinder is either stationary or rotating about its own axis. If the cylinder rotates in the presence of the singularities, then the stream function is taken to be

$$\Psi(r, \theta) = \psi(r, \theta) - k \log \frac{r}{a}, \quad k > 0.$$

Here, $\psi(r, \theta)$ refers to the stream function when the cylinder is stationary. The second term arises when the cylinder rotates about its axis. Below we refer to k as the rotation parameter. The negative sign in front of the second term indicates the rotation in the counterclockwise direction for our purposes below. We provide the discussion for exterior flows in Sec. III and for interior flows in Sec. IV.

III. EXTERIOR FLOWS

The solutions for various singularity driven flows may be obtained by the Fourier expansion method. We skip the details and present the exact solutions in each case. The closed form solutions are then used to illustrate the flow topologies in each case. For our purposes, the center of the cylinder is taken to be the origin of the coordinate system and the primary singularities are assumed to lie on the x axis but outside the cylinder $r>a$. Next, we consider various singularity induced flows past a cylinder.

A. Pair of rotlets

We consider a pair of rotlets of strengths F and F' positioned at $(r,\theta)=(c,0)$, and $(r,\theta)=(c',\pi)$, respectively. Here $c,c'>a$. The stream function corresponding to these rotlets in an unbounded flow is

$$\psi_0 = F(\log R) + F'(\log R'), \tag{8}$$

where

$$R^2 = r^2 - 2cr\cos\theta + c^2, \quad R'^2 = r^2 + 2c'r\cos\theta + c'^2.$$

Now the solution of Eq. (3) satisfying Eqs. (6) and (7) in the presence of two rotlets may be obtained by either the singularity method[15,18] or the Fourier series method.[17] The solution can also be derived using the boundary integral equation method.[22] Since the derivation is straightforward, we omit the details for the sake of brevity and give the final solution for the stream function:

$$\begin{aligned}\psi = {} & F\left[\log R - \log\left(\frac{cR_1}{a}\right) + \frac{a^2(a^2-c^2)}{c^4}\,\frac{(rc\cos\theta - a^2)}{R_1^2} + \frac{a^2}{c^4R_1^2}(r^2c^2\cos 2\theta - 2a^2rc\cos\theta + a^4) + \log\left(\frac{r}{a}\right) + \frac{r}{c}\cos\theta\right] \\ & + F'\left[\log R' - \log\left(\frac{c'R_1'}{a}\right) - \frac{a^2(a^2-c'^2)}{c'^4}\,\frac{(rc'\cos\theta + a^2)}{R_1'^2}\right. \\ & \left. + \frac{a^2}{c'^4R_1'^2}(r^2c'^2\cos 2\theta + 2a^2rc'\cos\theta + a^4) + \log\left(\frac{r}{a}\right) - \frac{r}{c'}\cos\theta\right],\end{aligned} \tag{9}$$

where

$$R_1^2 = r^2 - 2\frac{a^2}{c}r\cos\theta + \frac{a^4}{c^2},$$

$$R_1'^2 = r^2 + 2\frac{a^2}{c'}r\cos\theta + \frac{a^4}{c'^2}.$$

The image system for a rotlet located at $(c,0)$ consists of a rotlet, a potential-dipole, and a Stokes dipole at $(a^2/c,0)$ together with a rotlet at the origin and a uniform flow at infinity. The image system for the other rotlet located at (c',π) also consists of the same set of singularities as the previous one except that the direction of the uniform flow at infinity is reversed here. The image solution for a single rotlet was given independently by Dorrepaal *et al.*,[15] Avudainayagam,[18] and Smith.[23] If we take $F'=0$ and $a=1$ in Eq. (9), we obtain the solution for a single rotlet derived by these authors.

It is evident from Eq. (9) that for large r,

$$\psi \sim \left(\frac{F}{c} - \frac{F'}{c'}\right) r\cos\theta + (F+F')\log\left(\frac{r}{a}\right) + O(1), \tag{10}$$

which shows that the far-field behavior is that of uniform flow with speed $[(F/c)-(F'/c')]$. It is interesting to note that for a pair of rotlets with equal strengths and with $c=c'$, the far-field uniform flow vanishes. In this case the flow behavior changes significantly. We return to the discussion of flow patterns later in this subsection.

Since expression (9) corresponds to a force-free representation for a pair of line rotlets, the force acting on the cylinder is zero. However, the torque acting on the cylinder need not be zero. The torque may be calculated from the fact that it is $4\pi\mu$ times the strength of the image rotlet at the origin. Therefore, it follows from Eq. (9) that the torque in the present case is $4\pi\mu(F+F')$. The torque vanishes if the rotlets have opposite strengths.

It is worth mentioning that the corresponding solution for a plane boundary can be obtained from Eq. (9) in the limit of large radius. The no-slip plane boundary in this case becomes $x=0$ and the fluid occupies the region $x>0$. We first derive the limiting case for a single rotlet located in the vicinity of the plane boundary $x=0$. If a,c both approach infinity while $(c-a)\to h_1$, then Eq. (9), with $F'=0$, after some simplification reduces to

$$\psi(x,y) = F\left(\log R - \log R_1 + \frac{2x(x+h_1)}{R_1^2}\right) \tag{11}$$

with $R^2=(x-h_1)^2+y^2$ and $R_1^2=(x+h_1)^2+y^2$. The above solution corresponds to the case of a single rotlet situated near a rigid plane boundary. If we take $h=1$ and replace x by

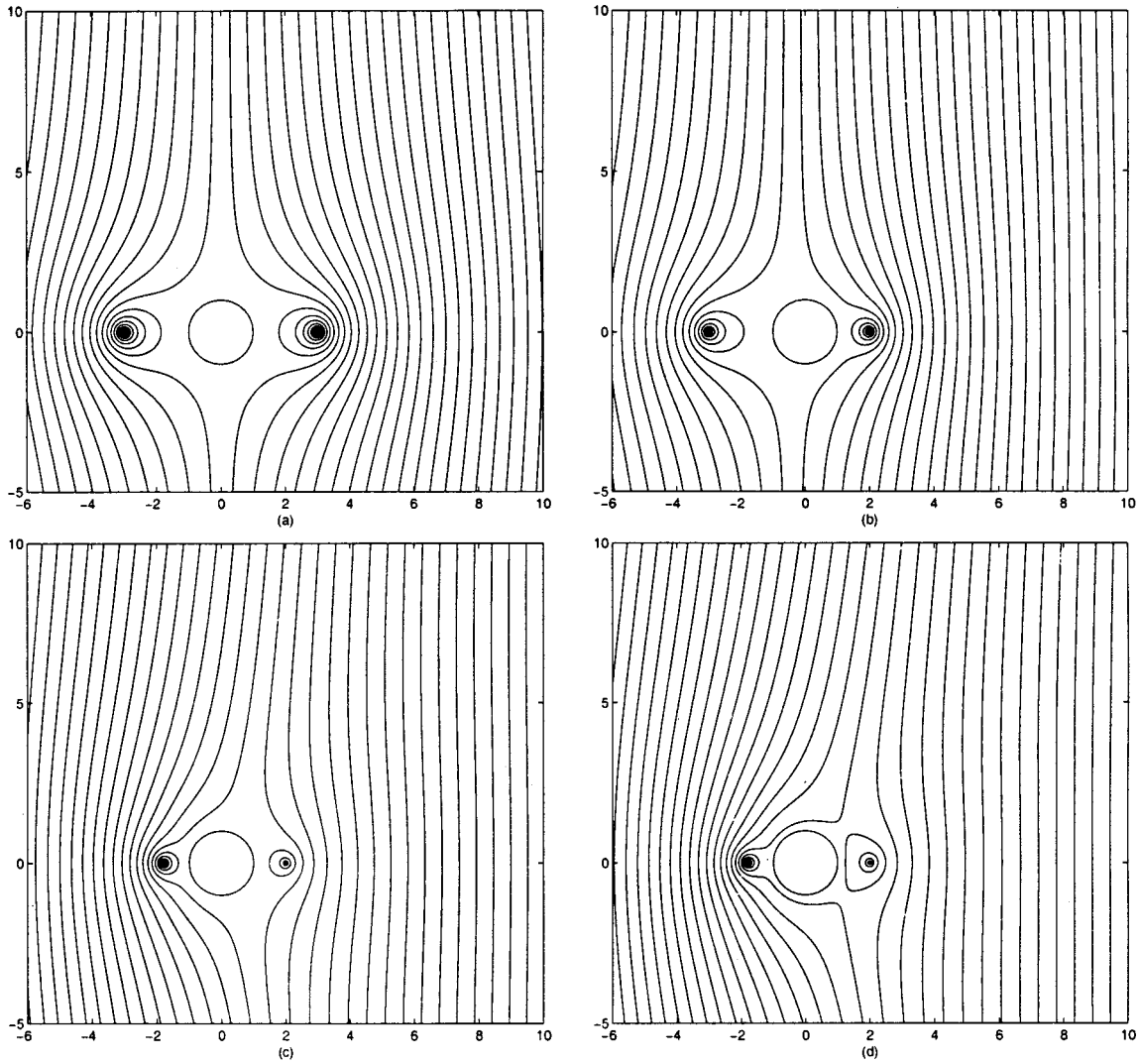

FIG. 1. Exterior flows: Streamlines for a pair of rotlets with equal strengths but of opposite sign (''opposite rotlets'') for their various locations in the presence of a cylinder. (a) $c=a+2$, $c'=a+2$, $k=0.0$; (b) $c=a+1$, $c'=a+1.5$, $k=0.0$; (c) $c=a+1$, $c'=a+0.9$, $k=0.5$; (d) $c=a+1$, $c'=a+0.8$, $k=1.1$.

y in the expression (11), we recover the solution due to Ranger.[24] Similar limiting procedure with $F'\neq 0$ in Eq. (9) leads to a solution which is not physical. This is because the rotlet with strength F' in this case is located in the region $(x<0)$ not occupied by the fluid. However, by a suitable transformation of the y coordinate (after taking the limits), the solution for a pair of rotlets located in the vicinity of a plane boundary may be obtained. To this end, we first let a,c, c' all approach infinity while $(c-a)\to h_1$ and $(c'-a)\to h_1'$ in Eq. (9). In the resulting expression, we make the transformation $y\to(y-a_1)$ in the terms multiplied by F and $y\to(y+a_1')$ in the terms multiplied by F' and replace h_1' by $-h_1'$. This yields

$$\psi(x,y)=F\left(\log R_t-\log R_{1t}+\frac{2x(x+h_1)}{R_{1t}^2}\right)+F'\left(\log R_t'-\log R_{1t}'+\frac{2x(x+h_1')}{R_{1t}'^2}\right), \qquad (12)$$

where $R_t^2=(x-h_1)^2+(y-a_1)^2$ and $R_{1t}^2=(x+h_1)^2+(y-a_1)^2$. By replacing h_1,a_1 by $h_1',-a_1'$ in R_t,R_{1t}, the expressions for R_t',R_{1t}' may be written down in a similar fashion. The above solution corresponds to a pair of rotlets located at (h_1,a_1), $(h_1',-a_1')$ near a plane boundary.

We now turn our attention to the flow streamlines for a pair of rotlets in the presence of a cylinder. The streamlines are sketched using Eq. (9) for different values of the parameters F, F', c, c', and k (rotation parameter). Here and in subsequent sections, we use the terminology ''a pair of opposite rotlets/stokeslets'' to refer to two rotlets/stokeslets of equal strengths but of different sign. We also use the terminology ''a pair of equal rotlets/stokeslets'' to refer to two rotlets/stokeslets of equal strengths and of same sign. In this case, both the rotlets/stokeslets can have either positive or negative sign. We have considered only the case with positive sign in the present study. The counterclockwise rotation is considered in the case of a cylinder rotating in the presence of rotlets/stokeslets. The term ''equidistance'' is used to

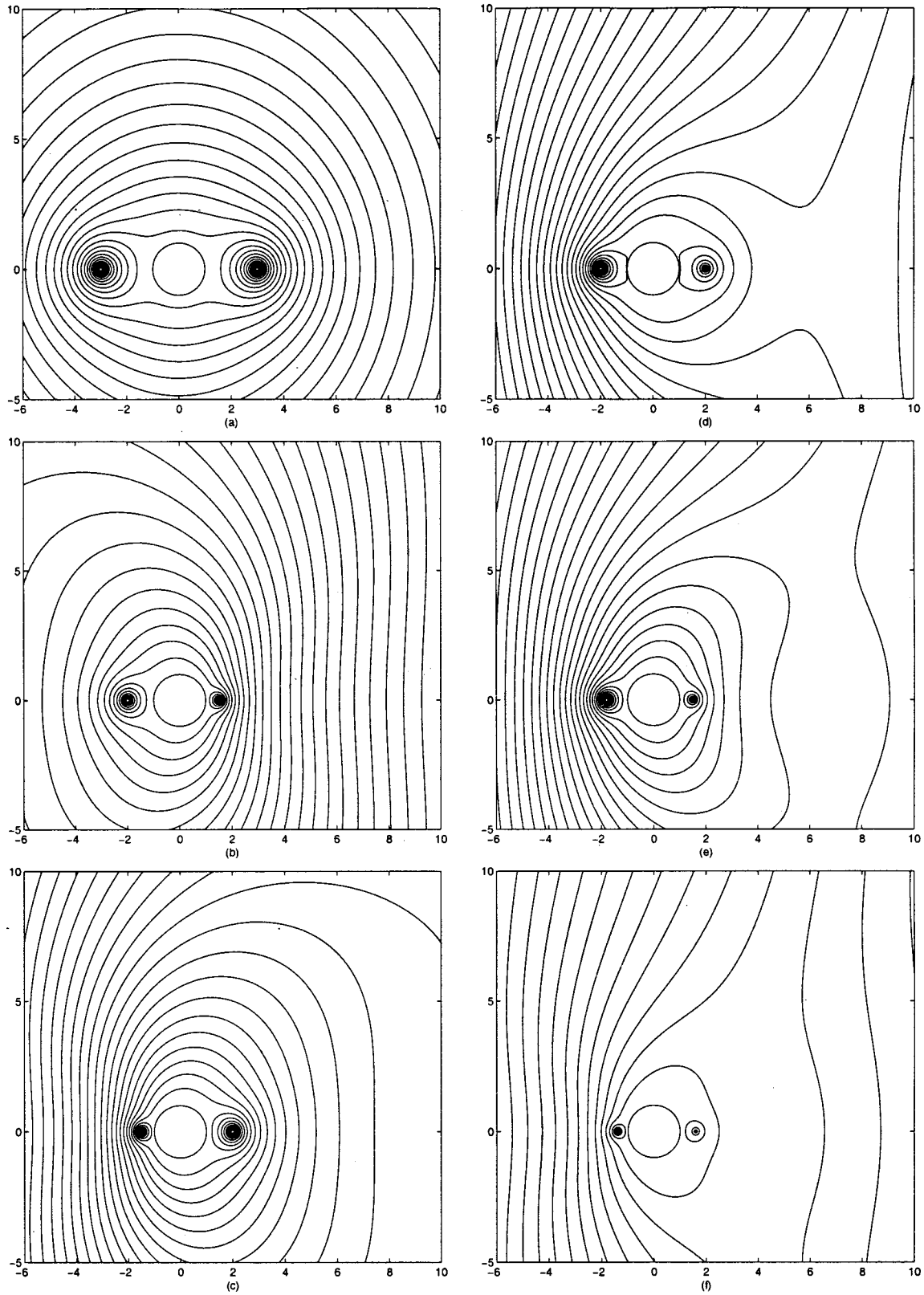

FIG. 2. Exterior flows: Streamlines for a pair of rotlets with (i) equal strengths ($F=F'$) and (ii) different strengths ($F'=2F$) in the absence of rotation. (i) $F'=F$: (a) $c=a+2$, $c'=a+2$; (b) $c=a+0.5$, $c'=a+1$; (c) $c=a+1$, $c'=a+0.5$; (ii) $F'=2F$: (d) $c=a+1$, $c'=a+1$; (e) $c=a+0.5$, $c'=a+0.8$; (f) $c=a+0.6$, $c'=a+0.4$.

refer to two rotlets/stokeslets located at equal distance ($c=c'$) from the center of the cylinder along the x-axis. The cases with different strengths of the primary singularities are also considered and explained at appropriate places. Below we discuss the streamline patterns for a pair of rotlets in the presence of a cylinder.

In Fig. 1 we have plotted the streamlines for a pair of opposite rotlets ($F'=-F=1$) for various locations of the

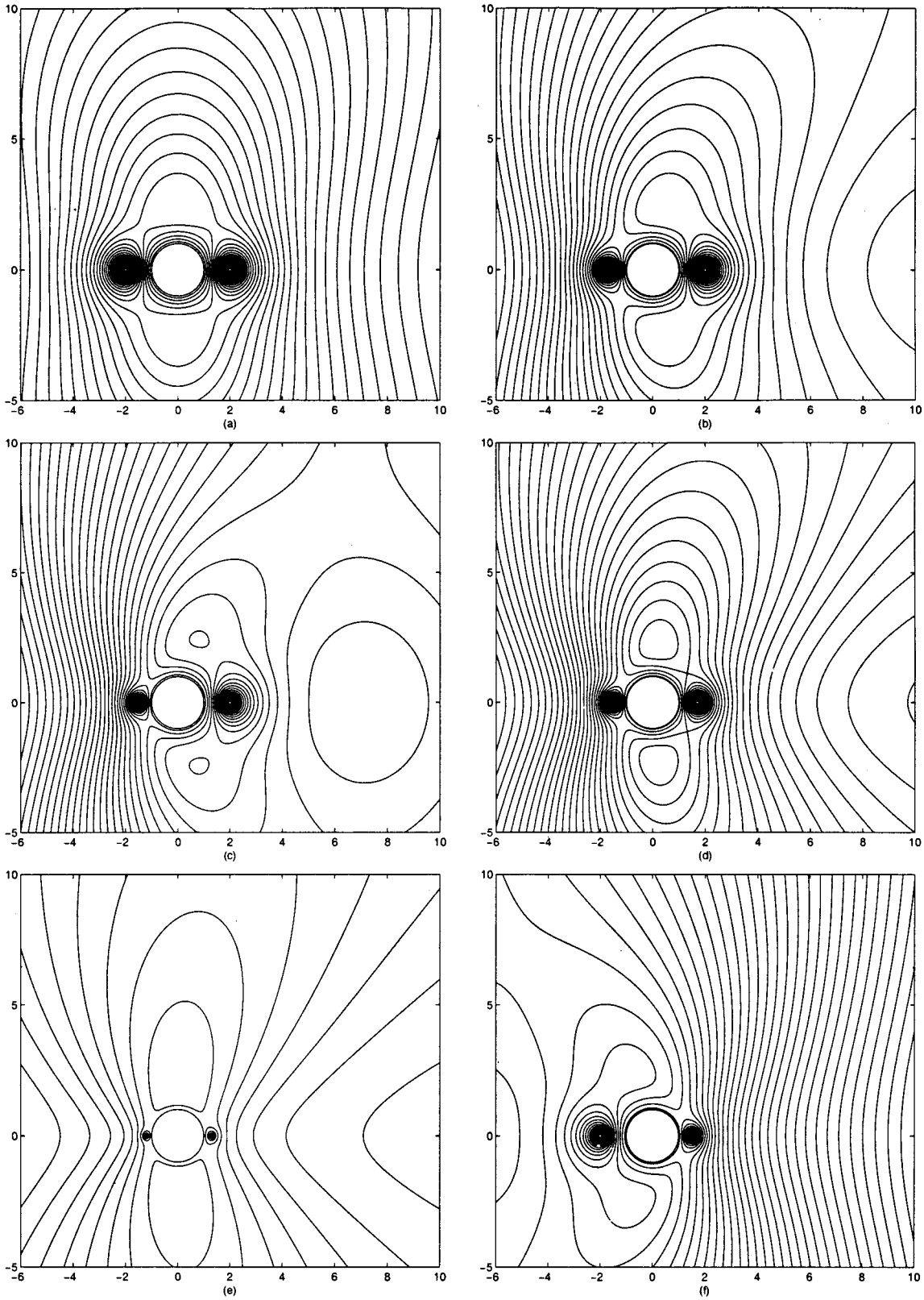

FIG. 3. Exterior flows: Streamlines for a pair of equal rotlets for their various locations with rotation parameter $k=1.1$. (a) $c=a+1$, $c'=a+1$; (b) $c=a+1$, $c'=a+0.7$; (c) $c=a+1$, $c'=a+0.5$; (d) $c=a+0.7$, $c'=a+0.5$; (e) $c=a+0.3$, $c'=a+0.2$; (f) $c=a+0.5$, $c'=a+1$.

primary singularities. In the absence of rotation, the flow-streamlines are closed in the neighborhood of the singularities and are parallel to the y-axis at distances far from them. In other words, the flow is uniform in the y-direction [see Figs. 1(a)–1(b)] far from the cylinder. The locations of rotlets influence the flow patterns very little. However, rotation of the cylinder changes the flow pattern noticeably as evident from Figs. 1(c)–1(d). When $k=1.1$, eddies of semicircular

shape appear around the rotlet which is farther from the cylinder. The flow is uniform far away from the cylinder as before and is not affected by the rotation.

Figure 2 illustrates the cases of a pair of rotlets of (i) equal strengths, i.e., equal rotlets [Figs. 2(a)–2(c)] and (ii) different strengths ($F'=2F$) and of same sign [Figs. 2(d)–2(f)]. In the case of rotlets having equal strengths and for $c=c'$, the terms due to uniform flow cancels and the far-field is no longer uniform. The flow streamlines are closed and appear as a single set of eddies enclosing the cylinder and rotlets [Fig. 2(a)]. The enclosing streamline pattern was also noticed earlier in the case of two rotating cylinders.[15] For $c>c'$ or $c>c'$, the closed streamline pattern surrounding the cylinder and rotlets changes its size and shape as shown in Figs. 2(b)–2(c). The existence of the eddy and the uniform flow in the far-field are due to the interaction of the two rotlets. In the case of rotlets having different strengths and of same sign, the uniform flow always exists for all values of c and c' [Figs. 2(d)–2(f)]. Here again, shape of the eddy structure changes considerably with various rotlet locations.

The streamlines for a pair of equal rotlets with cylinder rotation are sketched in Fig. 3 for various locations of the rotlets. The cylinder rotates with $k=1.1$. In this case the streamlines show very interesting flow patterns. If the rotlets are located equidistant from the cylinder, eddies of different shapes appear in the flow field, as can be seen from Fig. 3(a). Two sets of eddies surrounding the rotlets, one surrounding cylinder, and the other one surrounding the cylinder and rotlets, appear in the flow field. On the other hand, if the rotlets are located at nonequidistant positions, two sets of eddies are formed of which one is nearly circular in shape and the other has unusual shape [Figs. 3(b)–3(d)]. The sizes and shapes of these eddies change significantly with c and c'. Figure 3(d) further shows that there are two stagnation points near the rotlet which is farther from the cylinder. The closed separatrix through these two stagnation points enclose three eddies. These interesting features disappear if the locations of the primary rotlets are changed. For instance, if the rotlets are moved much closer to the cylinder, the unusual eddy structure disappears and a pair of symmetrical eddies enclosed in a single larger eddy appears [Fig. 3(e)]. The unusual eddies seem to appear near the rotlet that is farther from the cylinder [see Figs. 3(c), 3(f)].

B. Pair of stokelets with their axes along *x*-direction

Now we consider a pair of stokeslets of strengths F and F' positioned at $(r,\theta)=(c,0)$, and $(r,\theta)=(c',\pi)$, respectively. Here $c,c'>a$. The axes of these stokeslets are taken to be along the x-direction. The stream function corresponding to this pair of stokeslets in an unbounded flow is

$$\psi_0=[F(\log R)+F'(\log R')]r\sin\theta. \tag{13}$$

The solution of Eq. (3) satisfying Eqs. (6) and (7) in the presence of the cylinder and the pair of stokeslets is

$$\psi(r,\theta)=F\left[r\sin\theta\left(\log R-\log\left(\frac{cR_1}{a}\right)-\frac{a^2(c^2-a^2)^2}{2c^4R_1^2}+\frac{(c^2-a^2)}{2c^2}\right)+\frac{a^2(c^2-a^2)}{2c^5R_1^2}(r^2c^2\sin 2\theta-2a^2rc\sin\theta)\right]$$
$$+F'\left[r\sin\theta\left(\log R'-\log\left(\frac{c'R_1'}{a}\right)-\frac{a^2(c'^2-a^2)^2}{2c'^4R_1'^2}+\frac{(c'^2-a^2)}{2c'^2}\right)+\frac{a^2(c'^2-a^2)}{2c'^5R_1'^2}(r^2c'^2\sin 2\theta-2a^2rc'\sin\theta)\right]. \tag{14}$$

The image system for a stokeslet at $(c,0)$ consists of a stokeslet, a potential-dipole, and a Stokes-dipole at $(a^2/c,0)$ together with a uniform flow along the x-direction at infinity. For a stokeslet at (c',π), the image system is the same as the previous one with their strengths depending on F',c', and a. At a large distance from the cylinder, we have

$$\psi\sim\left[F\left(\frac{c^2-a^2}{2c^2}-\log\left(\frac{c}{a}\right)\right)+F'\left(\frac{c'^2-a^2}{2c'^2}-\log\left(\frac{c'}{a'}\right)\right)\right]r\sin\theta, \tag{15}$$

which corresponds to a uniform stream in the positive x-direction. The speed of the uniform stream depends on the singularity strengths F,F', the radius a, and the singularity locations c,c'. For a pair of opposite stokeslets (i.e., $F'=-F$) with $c=c'$, the uniform flow vanishes. Since there is no rotlet at the origin [see Eq. (14)], the torque in this case is zero.

We now deduce the limiting case for a pair of stokeslets located in the vicinity of a plane boundary. This may be obtained by the similar procedure [see Sec. III A, the discussion just above Eq. (12)] described for a pair of rotlets. In Eq. (14), we let a,c,c' all three approach infinity while $(c-a)\to h_1$, $(c'-a)\to h_1'$. The resulting expression, after using the transformation given in the case of a pair of rotlets, becomes

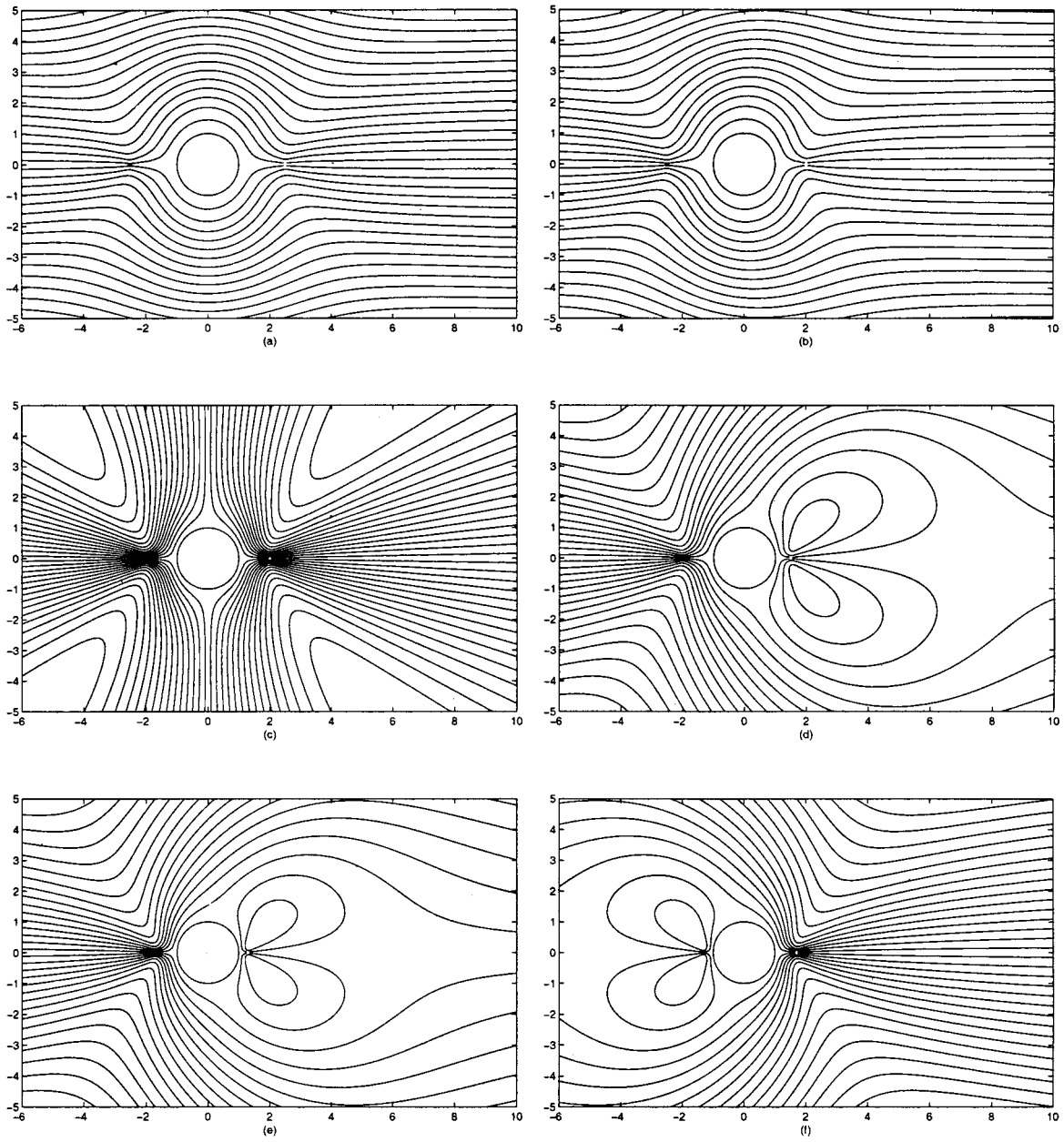

FIG. 4. Exterior flows: Streamlines for a pair of stokeslets along the x-direction for their various locations in the absence of cylinder rotation. (i) Equal stokeslets: (a) $c=a+1.5$, $c'=a+1.5$; (b) $c=a+1$, $c'=a+1.5$; (ii) opposite stokeslets: (c) $c=a+1$, $c'=a+1$; (d) $c=a+0.5$, $c'=a+1$; (e) $c=a+0.3$, $c'=a+0.7$; (f) $c=a+0.7$, $c'=a+0.3$.

$$\psi(x,y)=F(y-a_1)\left(\log R_t-\log R_{1t}+\frac{2xh_1}{R_{1t}^2}\right)+F'(y+a_1')\left(\log R_t'-\log R_{1t}'+\frac{2xh_1'}{R_{1t}'^2}\right). \quad (16)$$

The above stream function represents the solution for the flow due to a pair of stokeslets in the presence of a plane boundary. The solution for a pair of equal stokeslets in the presence of a plane boundary was derived by Liron and Blake.[25] For $F=F'$, $h_1=h_1'$, $a_1=a_1'$, Eq. (16) can be shown to be equivalent to the result obtained in Ref. 25. If we take $F'=0$ in Eq. (16), we get the result for a single stokeslet in the presence of a plane boundary.[26]

The streamlines due to a pair of stokeslets in the absence of rotation are plotted for various values of c and c' in Fig. 4 using Eq. (14). In the case of equal stokeslets, the far-field flow is uniform for different locations of the stokeslets [Figs. 4(a)–4(b)]. On the other hand, in the case of opposite stokeslets, the uniform flow disappears for $c=c'$ [see Fig. 4(c)]. The streamlines emanating from each stokeslet strongly oppose each other in this case. For $c\neq c'$, a pair of symmetrical toroidal eddies are formed near the stokeslet closer to the cylinder, as shown in Figs. 4(d)–4(f). The size of this eddy structure changes according to the location of the two stokeslets.

In Fig. 5 the streamlines are shown for a pair of stokes-

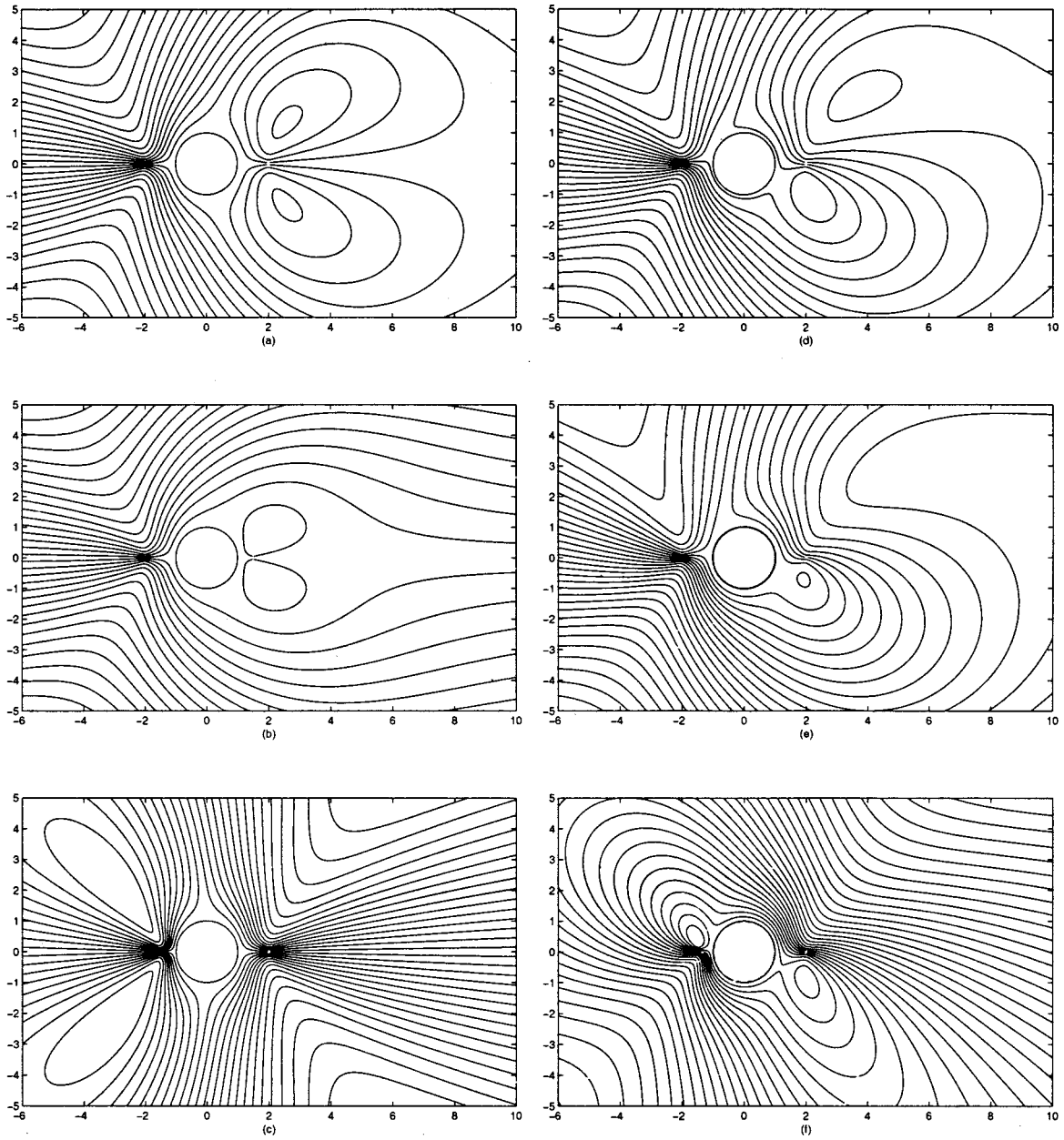

FIG. 5. Exterior flows: Streamlines for a pair of stokeslets of different strengths and of different sign with and without rotation. The axes of the stokeslets are in the x-direction and we have chosen $F'=-2F$. (a) $c=a+1$, $c'=a+1$, $k=0.0$; (b) $c=a+0.5$, $c'=a+1$, $k=0.0$; (c) $c=a+1$, $c'=a+0.5$, $k=0.0$; (d) $c=a+1$, $c'=a+1$, $k=0.5$; (e) $c=a+1$, $c'=a+1$, $k=0.9$; (f) $c=a+1$, $c'=a+0.5$, $k=0.9$.

lets with different strengths and of opposite sign for the cases (i) with rotation and (ii) without rotation. The strength of the stokeslet located at (c',π) is chosen as $F'=-2F$. In both cases, a symmetric pair of eddies (symmetrical about the x-axis) appears. In the absence of rotation, size *and shape* of the eddy structure *are* altered by the location of the stokeslets [Figs. 5(a)–5(c)]. In the presence of rotation, the size, shape, and the location of the eddy structure change remarkably as in Figs. 5(d)–5(e). When $k=0.9$ and the stokeslets are located equidistant from the cylinder, the eddy on the positive side of y-axis is destroyed and the one on the negative side is distorted [Fig. 5(e)]. When $k=0.9$ and the stokeslets are located at nonequidistant positions, the symmetric pair of toroidal eddies appears diagonally opposite to each other [Fig. 5(f)]. The rotation parameter and the stokeslet locations completely dictate the eddy locations, its size, and shape in all the situations.

C. Pair of stokelets with their axes along the *y*-direction

Now we consider a pair of stokeslets of strengths F and F' positioned at $(r,\theta)=(c,0)$, and $(r,\theta)=(c',\pi)$, respectively. Here $c,c'>a$. The axes of these stokeslets are taken to be along the y-direction. The stream function corresponding to this pair of stokeslets in an unbounded flow is

$$\psi_0=-F(r\cos\theta-c)\log R+F'(r\cos\theta+c')\log R'. \qquad (17)$$

The solution to Eq. (3) satisfying Eqs. (6) and (7) in the presence of the cylinder and the stokeslets is

$$\psi(r,\theta)=F\Bigg[-(r\cos\theta-c)\log R+\left(r\cos\theta-\frac{a^2}{c}\right)\log\left(\frac{cR_1}{a}\right)+\frac{(c^2-a^2)}{c}\log(cR_1)+\frac{(c^2-a^2)}{c}\log\left(\frac{r}{a}\right)-\frac{a^2(c^2-a^2)^2}{2c^5}\frac{(rc\cos\theta-a^2)}{R_1^2}+\frac{a^2(c^2-a^2)}{2c^5R_1^2}(r^2c^2\cos 2\theta-2a^2r\cos\theta+a^4)+\frac{c^2-a^2}{2c^2}r\cos\theta\Bigg]+F'\Bigg[(r\cos\theta+c')\log R_1'-\left(r\cos\theta+\frac{a^2}{c'}\right)\log\left(\frac{c'R_1'}{a}\right)+\frac{(c'^2-a^2)}{c'}\log(c'R_1')+\frac{(c'^2-a^2)}{c'}\log\left(\frac{r}{a}\right)+\frac{a^2(c'^2-a^2)^2}{2c'^5}\frac{(rc'\cos\theta+a^2)}{R_1'^2}+\frac{a^2(c'^2-a^2)}{2c'^5R_1'^2}(r^2c'^2\cos 2\theta+2a^2rc'\cos\theta+a^4)-\frac{c'^2-a^2}{2c'^2}r\cos\theta\Bigg]. \tag{18}$$

The image system for a stokeslet at $(c,0)$ consists of a stokeslet, a rotlet, a potential-dipole, and a Stokes-dipole at $(a^2/c,0)$ together with a rotlet at the origin and a uniform flow along the y-direction at infinity. For a stokeslet at (c',π), the image system is the same as the previous one except that the direction of the uniform flow is reversed. At a large distance from the cylinder, we have

$$\psi\sim\left[F\left(\frac{c^2-a^2}{2c^2}+\log\left(\frac{c}{a}\right)\right)-F'\left(\frac{c'^2-a^2}{2c'^2}+\log\left(\frac{c'}{a}\right)\right)\right]r\cos\theta, \tag{19}$$

which corresponds to a uniform stream in the y-direction. The speed of this uniform stream also depends on F, F', the radius a, and the singularity locations as in the previous case. As in the case of rotlets, the uniform stream vanishes for two equal stokeslets along the y-direction with $c=c'$. The torque acting on the cylinder can be obtained from the force-free representation Eq. (17) and is given by

$$T=4\pi\mu\left[F\frac{c^2-a^2}{c}+F'\frac{c'^2-a^2}{c'}\right]. \tag{20}$$

The torque depends on the location of the primary singularities and the radius of the cylinder. It vanishes if the stokeslets have the opposite strengths (i.e., $F'=-F$) and are equidistant from the cylinder on its either side along the x-axis.

In the limit a, c, and c' approach infinity while $(c-a)\to h_1$, and $(c'-a)\to h_1'$ and using the procedure described in the case of a pair of rotlets, Eq. (18) becomes

$$\psi(x,y)=F\left[(h_1-x)(\log R_t-\log R_{1t})+\frac{2xh_1(x+h_1)}{R_{1t}^2}\right]+F'\left[(h_1'-x)(\log R_t'-\log R_{1t}')+\frac{2xh_1'(x+h_1')}{R_{1t}'^2}\right]. \tag{21}$$

The above expression represents the solution for the flow due to a pair of stokeslets along the y-direction near a plane boundary. The solution for a pair of opposite stokelets was derived by Liron and Blake.[25] When $F'=-F$, $h_1=h_1'=1$, $a_1=a_1'$, Eq. (21) can be shown to be equivalent to the result obtained in Ref. 25.

The streamlines for a pair of stokeslets along the y-direction are plotted for various values of c and c' in Fig. 6 using Eq. (18). In the case of two equal stokeslets at equidistant positions, the flow field is dominated by the uniform stream as noticed from Figs. 6(a)–6(b). In the case of opposite stokeslets, eddies appear surrounding the cylinder, and also surrounding both the cylinder and the stokeslets [see Fig. 6(c)]. For nonequidistant positions, eddies enclosing the cylinder and the stokeslets appear. Moreover, another set of eddies near the stokeslet closer to the cylinder also appear, as shown in Figs. 6(d)–6(f). The size and shape of this eddy structure changes significantly with the location of the stokeslets.

In Fig. 7 we have sketched the streamline patterns for the case of two stokeslets with rotation. When $k=0.9$, a symmetric pair of eddies appears in the neighborhood of the cylinder. One of these eddies is above the cylinder and the other is below and both are encapsulated in a single larger eddy [Fig. 7(a)]. If the stokeslets are placed equidistant from but closer to the cylinder, then the larger eddy disappears and the smaller pair isolates from each other [see Fig. 7(b)]. However, if the stokeslets are located closer to the cylinder at nonequidistant positions, then only a single set of eddy exists near the stokeslet closer to the cylinder, as evident from Fig. 7(c). The structure of the eddies for a different intensity of rotation (i.e., for different k) is shown in Figs. 7(d)–7(f).

IV. INTERIOR STOKES FLOWS

As in exterior flow, the center of the cylinder is taken to be the origin of the coordinate system and the primary singularities are assumed to lie on the x-axis but inside the cylinder $r<a$. The basic formulation for this interior Stokes

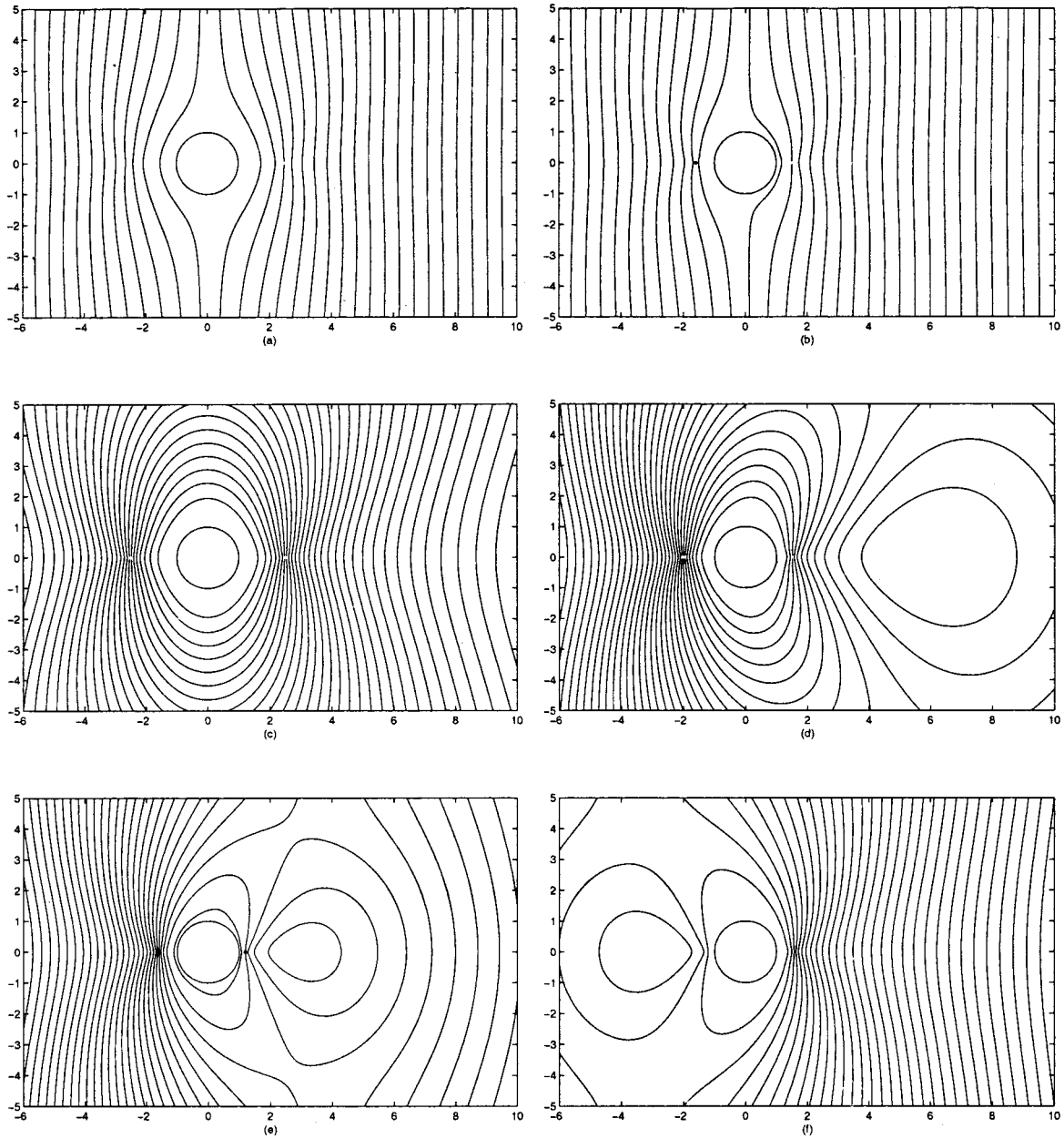

FIG. 6. Exterior flows: Streamlines for a pair of stokeslets along the y-direction in the absence of rotation. (i) Equal stokeslets: (a) $c=a+1.5$, $c'=a+1.5$; (b) $c=a+0.5$, $c'=a+0.6$; (ii) opposite stokeslets: (c) $c=a+1.5$, $c'=a+1.5$; (d) $c=a+0.5$, $c'=a+1.0$; (e) $c=a+0.2$, $c'=a+0.6$; (f) $c=a+0.6$, $c'=a+0.2$.

flow is similar to that of Sec. II. Therefore, we follow here the notations used in the previous sections. Furthermore, we adopt here the terminologies used in Sec. III. Below R, R', R_1, R_1' are given by the same formulas as in the exterior case. Now, we discuss the various singularity generated flows inside a cylinder.

A. Pair of rotlets

We consider a pair of rotlets of strengths F and F' positioned at $(r,\theta)=(c,0)$, and $(r,\theta)=(c',\pi)$, respectively. Here $c,c'<a$. The stream function corresponding to these rotlets in an unbounded flow is given in Eq. (8). The complete solution satisfying the equations of motion and the boundary conditions may be obtained by the use of Fourier expansion method. The final closed form solution is

$$\psi(r,\theta)=F\left[\log R-\log\frac{cR_1}{a}+\left(1-\frac{r^2}{a^2}\right)\frac{(a^4-c^2r^2)}{2c^2R_1^2}\right]+F'\left[\log R'-\log\frac{cR_1'}{a}+\left(1-\frac{r^2}{a^2}\right)\frac{(a^4-c^2r^2)}{2c^2R_1'^2}\right]. \tag{22}$$

It should be pointed out that the solution for a single rotlet inside a cylinder was derived independently by Ranger[24] and Meleshko *et al.*[27] Their solution may be recovered from Eq. (22) by putting $F'=0$. We now discuss different flow topologies in the case of a pair of rotlets.

In Fig. 8, the flow patterns are shown in the case of equal

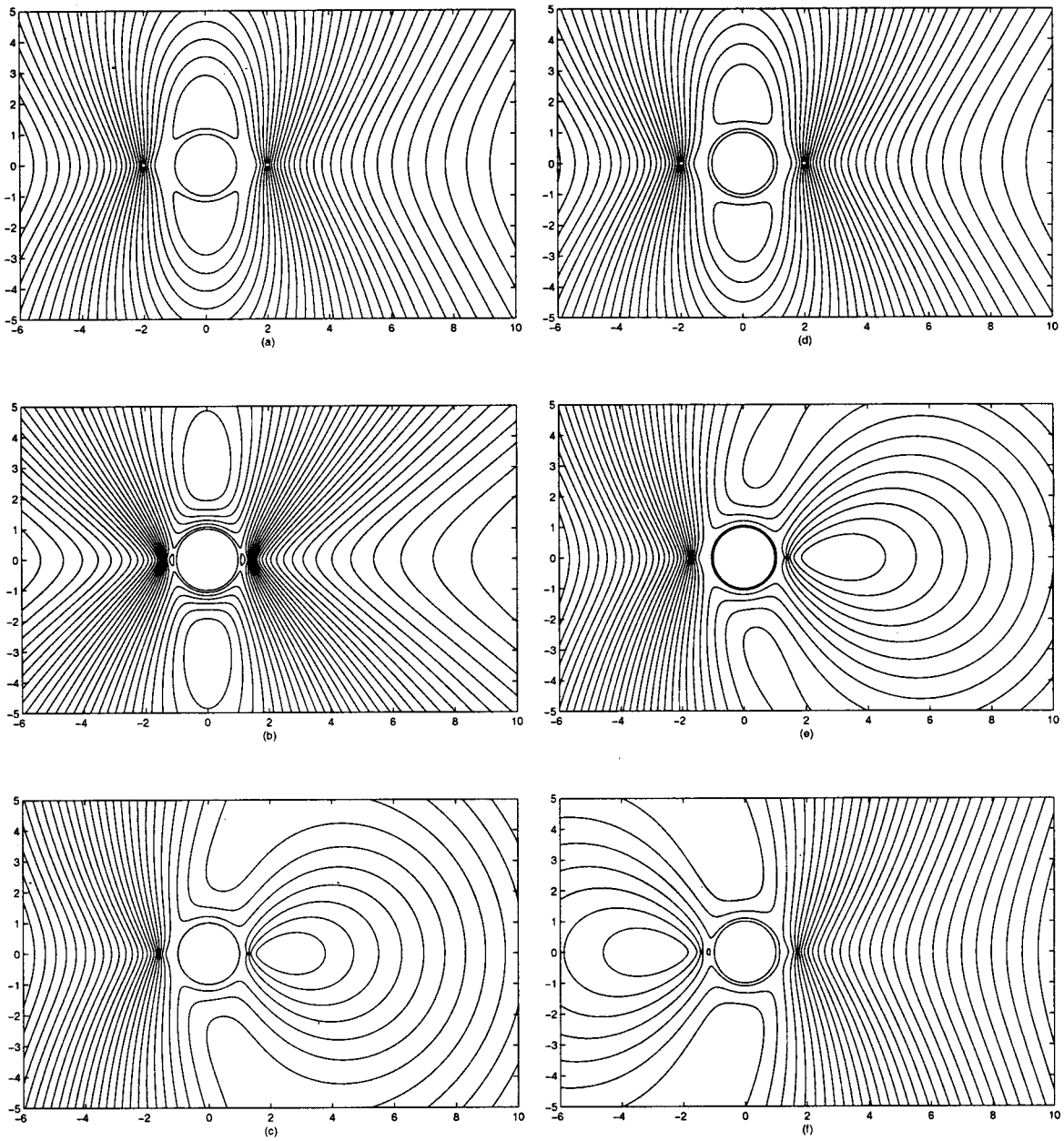

FIG. 7. Exterior flows: Streamlines for a pair of stokeslets along the y-direction for different values of the rotation parameter k. (i) $k=0.9$: (a) $c=a+1$, $c'=a+1$; (b) $c=a+0.4$, $c'=a+0.4$; (c) $c=a+0.3$, $c'=a+0.6$; (ii) $k=1.1$: (d) $c=a+1$, $c'=a+1$; (e) $c=a+0.4$, $c'=a+0.7$; (f) $c=a+0.7$, $c'=a+0.4$.

rotlets ($F=F'$) located at various equidistant positions in the absence of rotation. As seen from this figure, the distance parameters c and c' affect the flow patterns qualitatively. When the rotlets are positioned close to the center, a single larger eddy enclosing the rotlets and extending up to the cylinder wall appears as shown in Fig. 8(a). Of course, the fluid in the neighborhood of the rotlets exhibits a circulatory motion as expected. Interestingly, the latter nearly circular streamlines cross each other at the center giving birth to a double homoclinic orbit. If the two rotlets are moved away from the center according to equidistant criteria, the outer, larger eddy starts thinning in the middle, as shown in Fig. 8(b) for the case $c=c'=2.3$. As the rotlets are moved farther away, this thinning process continues due to the increase in the size of each of the attached eddies just above and below the neck of the larger eddy. A typical case of this scenario is shown in Fig. 8(c) where $c=c'=2.4$. Moving the rotlets even farther away from the center causes the larger eddy to split into two smaller eddies each around the rotlets, as shown in Fig. 8(b) where $c=c'=2.5$. Furthermore, the pair of attached eddies that existed before now connect at the center giving birth to a double homoclinic orbit. The double homoclinic orbit seems to disappear if the rotlets are moved even farther away from the center [see Fig. 8(e)]. Now the squeezing effect is reduced and the fluid around the center gets stretched along the y-axis, making the eddies around the rotlets thinner. If the rotlets are located very close to the wall, the fluid between them gets stretched along the x-direction as shown in Fig. 8(f). The core of the eddy (that occurs in the middle) has the shape of an ellipse.

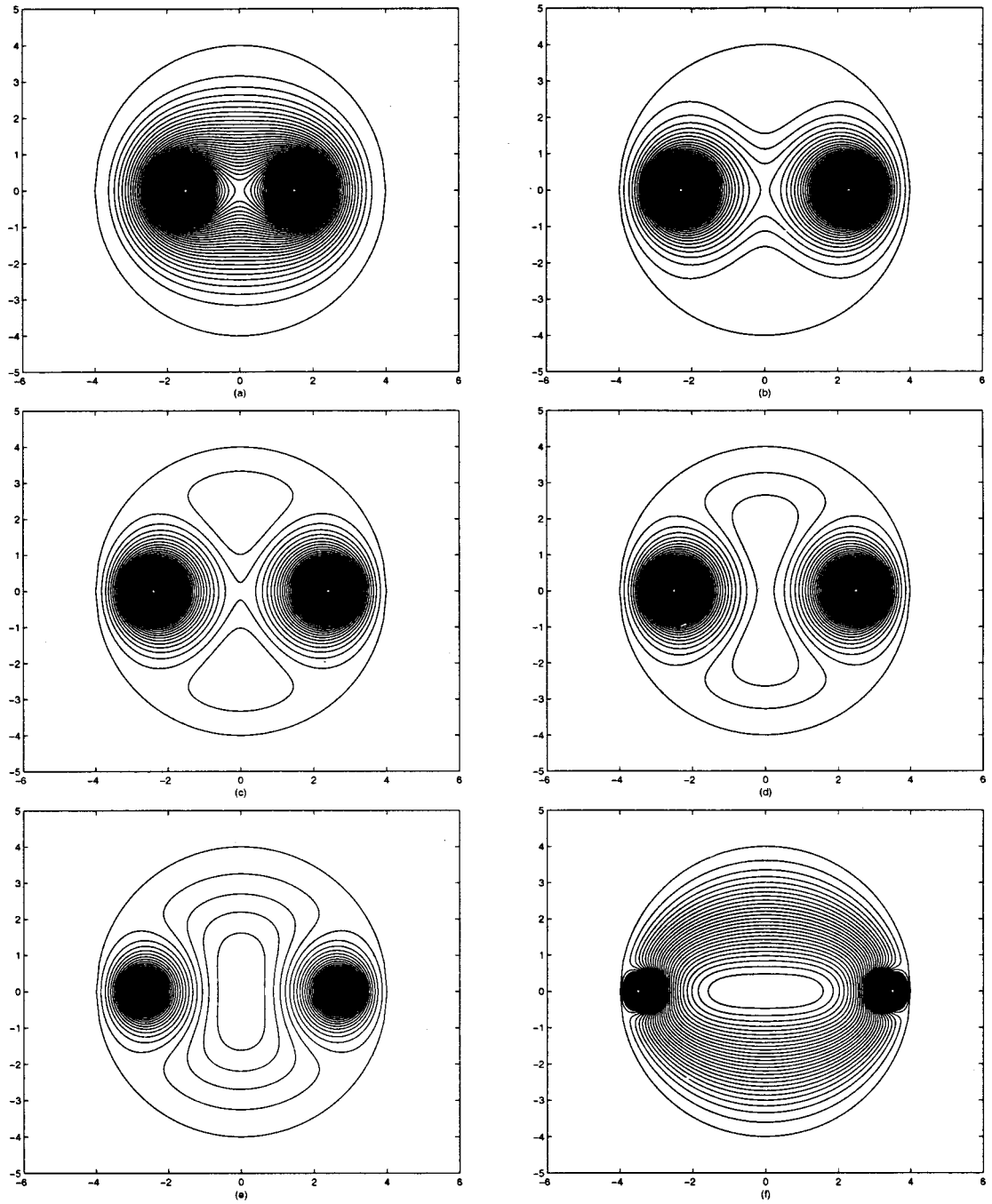

FIG. 8. Interior flows: Streamlines for a pair of equal ($F=F'=1$) and equidistant ($c=c'$) rotlets in the absence of rotation for several choices of rotlet locations. (a) $c=c'=1.5$; (b) $c=c'=2.3$; (c) $c=c'=2.4$; (d) $c=c'=2.5$; (e) $c=c'=2.7$; (f) $c=c'=3.5$.

Next we investigate the flow situations by fixing the rotlets at equidistant positions and allowing the cylinder to rotate in the counterclockwise direction. The flow topologies for various values of the rotation parameter k are shown in Fig. 9 keeping the rotlet locations fixed at $c=c'=1.5$. For small values of k, a larger eddy enclosing the rotlets and a pair of symmetric eddies (separated from the larger eddy) attached to the wall appear, as shown in Fig. 9(a). The rotation of the cylinder causes a circulatory motion of the fluid near the center. The circular streamlines around the rotlet cross each other just above and below the center yielding a pair of stagnation points lying on the y-axis (not shown in the figure). When $k=0.5$, the larger eddy breaks up into two eddies each around the rotlets, as seen in Fig. 9(b). The eddies attached to the wall now move closer to the center while the width of the circulatory flow region around the center increases. Further increase of k changes the size and shape of the different eddies [see Figs. 9(c)–9(d)]. The two symmetric eddies become a single larger eddy having a pair of cores on either side of the y-axis. This eddy has an unusual size and shape and seems to occur due to the cylinder rotation. For higher values of k, the shape of the unusual eddy changes significantly while the circulatory flow region expands. Some of this scenario is shown in Figs. 9(e)–9(f). The plots also show the thinning of the eddies around each rotlet as we increase the value of k. In all of these cases, the fluid close to

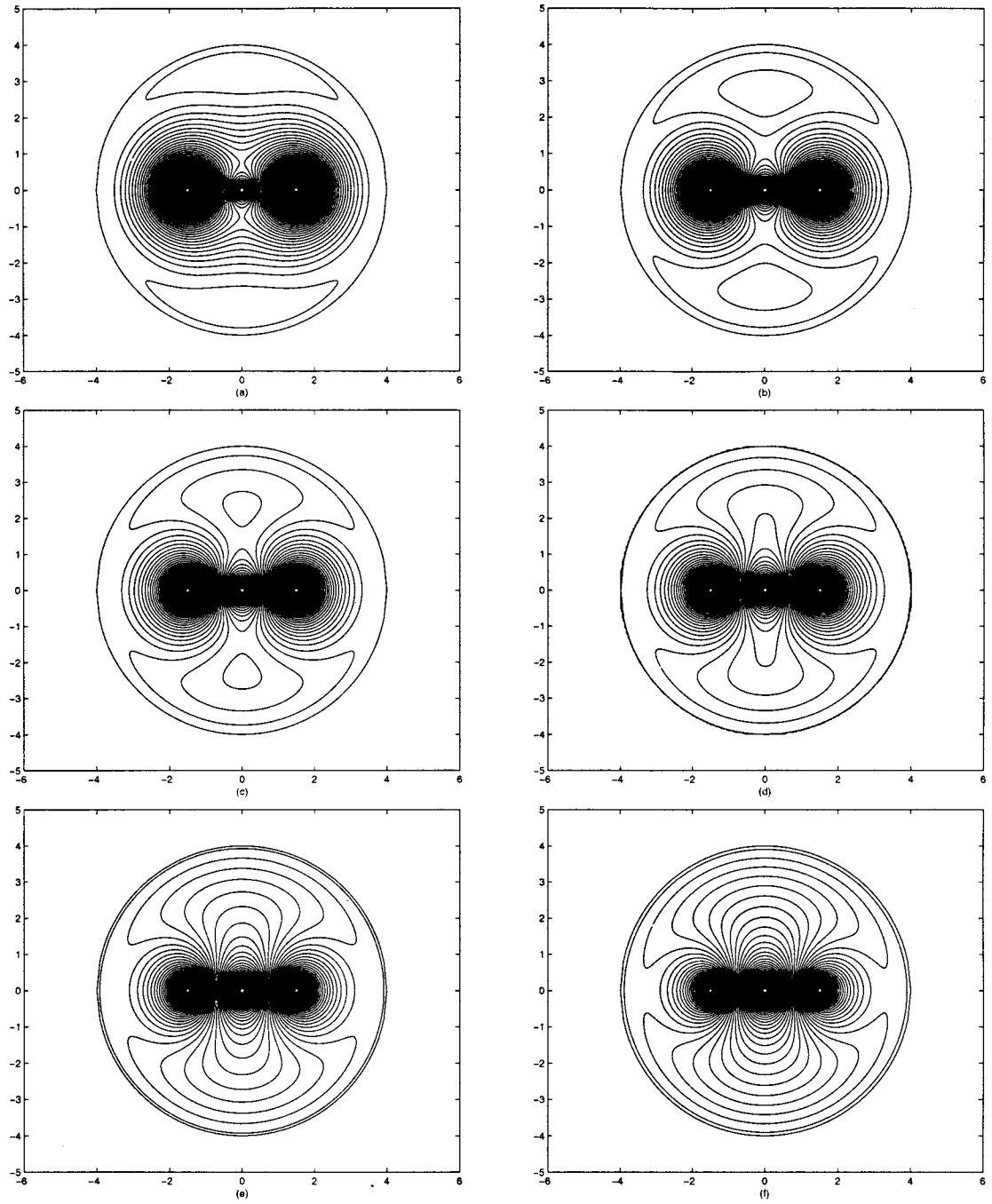

FIG. 9. Interior flows: Streamlines for a pair of equal ($F=F'=1$) and equidistant ($c=c'=1.5$) rotlets in the presence of counterclockwise rotation of the cylinder for several values of the rotation parameter k. (a) $k=0.3$; (b) $k=0.5$; (c) $k=0.6$; (d) $k=0.7$; (e) $k=0.9$; (f) $k=1.1$.

the wall exhibits a circulatory motion due to the rotation of the cylinder.

Figure 10 shows the flow patterns for a pair of equal rotlets ($F=F'=1$) for two different values of rotation parameter k and for various rotlet locations. When $k=0.5$ and $c=c'=1.0$ (equidistant rotlets), the flow structure shown in Fig. 10(a) is almost identical to that depicted in Fig. 9(a). The flow is more interesting for the same value of k but for nonequidistant positions of the rotlets. Figure 10(b) shows a typical case where $c=1.0$, and $c'=2.0$. In this case, an eddy around each rotlet and a circulatory flow region around the center appear. In addition, an outer eddy attached to most of the cylinder wall enclosing a pair of smaller eddies right above and below the center also appears. The streamline bounding this eddy is a heteroclinic orbit, as seen in this figure. Next, we show some streamline patterns for a higher speed of rotation of the cylinder in Figs. 10(c)–10(d) ($k=0.89$). Figures 10(c) and 10(d) correspond to the cases of equidistant and nonequidistant rotlets, respectively. In the equidistant case, the flow has a pair of stagnation points on the x-axis which are on a heteroclinic orbit. The fluid motion around the center and the rotlets in the present case are very similar to those depicted in Figs. 9(d)–9(e). In the nonequidistant case [Fig. 10(d)], a careful scrutiny of the streamlines

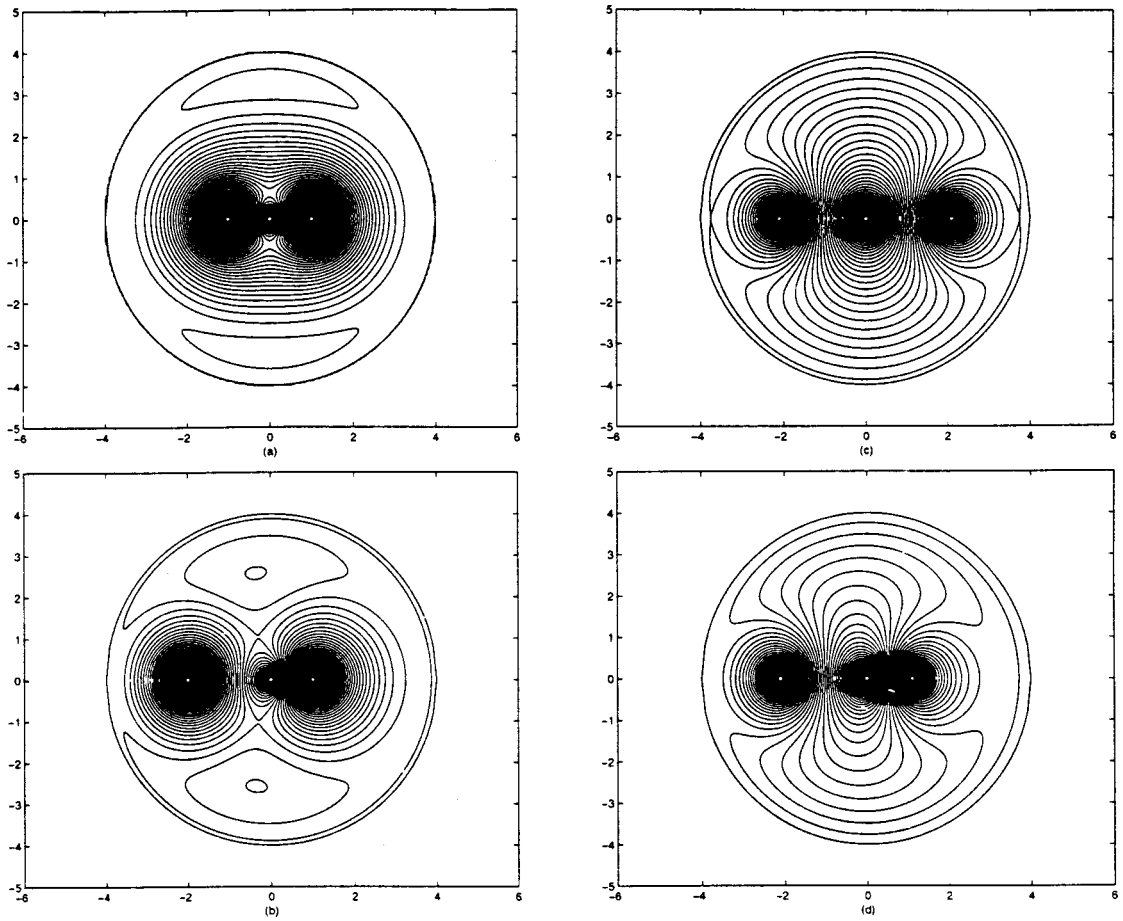

FIG. 10. Interior flows: Streamlines for a pair of equal rotlets ($F=F'=1$) in the presence of counterclockwise rotation of the cylinder for several values of k and rotlet locations. (i) $k=0.5$: (a) $c=c'=1.0$; (b) $c=1.0$, $c'=2.0$; (ii) $k=0.89$: (c) $c=c'=2.1$; (d) $c=1.1$, $c'=2.1$.

plotted shows that flow topology does not have heteroclinic orbit. Here some of the flow features resemble those of Fig. 10(b).

The flow topologies for a pair of opposite rotlets for two different locations for fixed $k=0.5$ are shown in Figs. 11(a)–11(b). The flow topologies for both equidistant and nonequidistant rotlets are almost the same as seen from these plots. A circular eddy appears in the neighborhood of the stokeslet which is on the positive x-axis. Further, an attached larger eddy enclosing the center and the stokeslet on the negative x-axis appears. The flow around the center is circulatory as expected. There appears to be a saddle stagnation point on the negative x-axis and perhaps a double homoclinic orbit. It may also be pointed out that some of the flow topologies found here are similar to those found in the vortex mixing flows.[21]

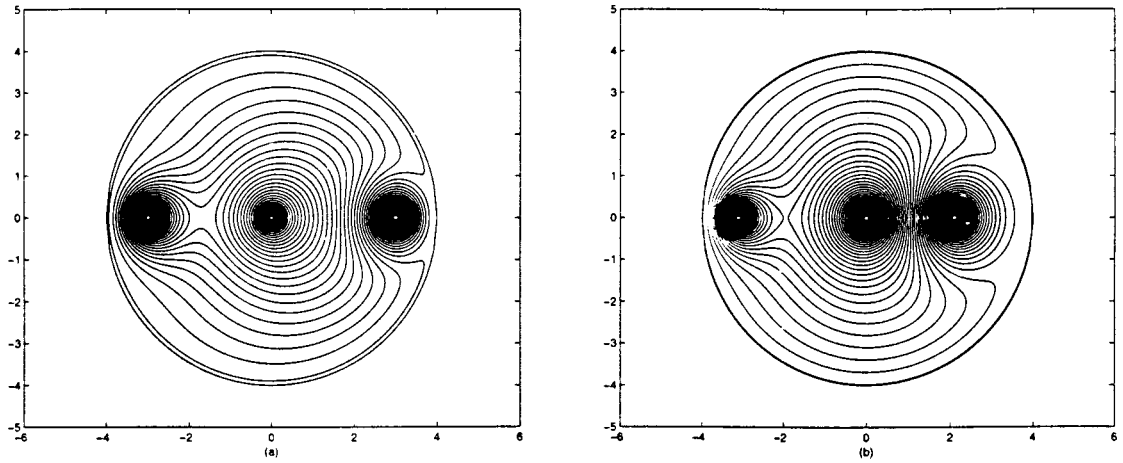

FIG. 11. Interior flows: Streamlines for a pair of opposite rotlets ($F=-F'=1$) in the presence of counterclockwise rotation of the cylinder for several values of k and rotlet locations. (a) $c=c'=3.0$; $k=0.5$; (b) $c=2.1$, $c'=3.1$, $k=-0.89$.

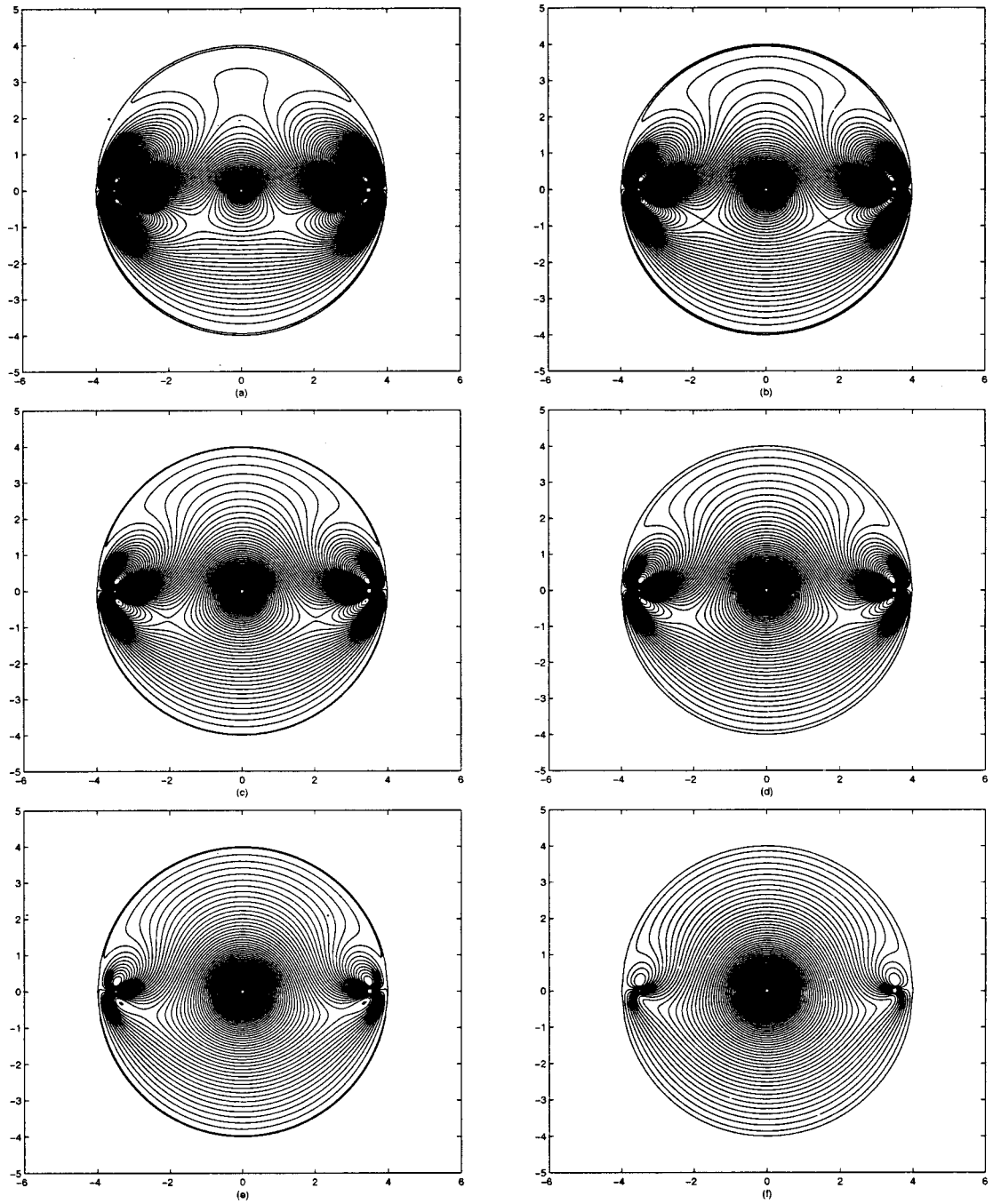

FIG. 12. Interior flows: Streamlines for a pair of equal ($F=F'=1$) and equidistant ($c=c'=3.5$) stokeslets with their axes along the x-direction in the presence of counterclockwise rotation of the cylinder for several values of k. (a) $k=0.05$; (b) $k=0.1$; (c) $k=0.15$; (d) $k=0.2$; (e) $k=0.4$; (f) $k=0.8$.

B. Pair of stokeslets with their axes along the *x*-direction

Now we consider a pair of stokeslets of strengths F and F' positioned at $(r,\theta)=(c,0)$, and $(r,\theta)=(c',\pi)$, respectively. Here $c,c'<a$. The axes of these stokeslets are taken to be along the x-direction. The stream function corresponding to this pair of stokeslets in an unbounded flow is given in Eq. (13). The complete solution satisfying the boundary conditions is

$$\psi(r,\theta)=F_1 r\sin\theta\left[\log R-\log\frac{cR_1}{a}+(r^2-a^2)\frac{(c^2-a^2)}{2c^2R_1^2}\right]+F'r\sin\theta\left[\log R'-\log\frac{cR_1'}{a}+(r^2-a^2)\frac{(c^2-a^2)}{2c^2R_1'^2}\right]. \tag{23}$$

The solution for a single stokeslet located inside a cylinder

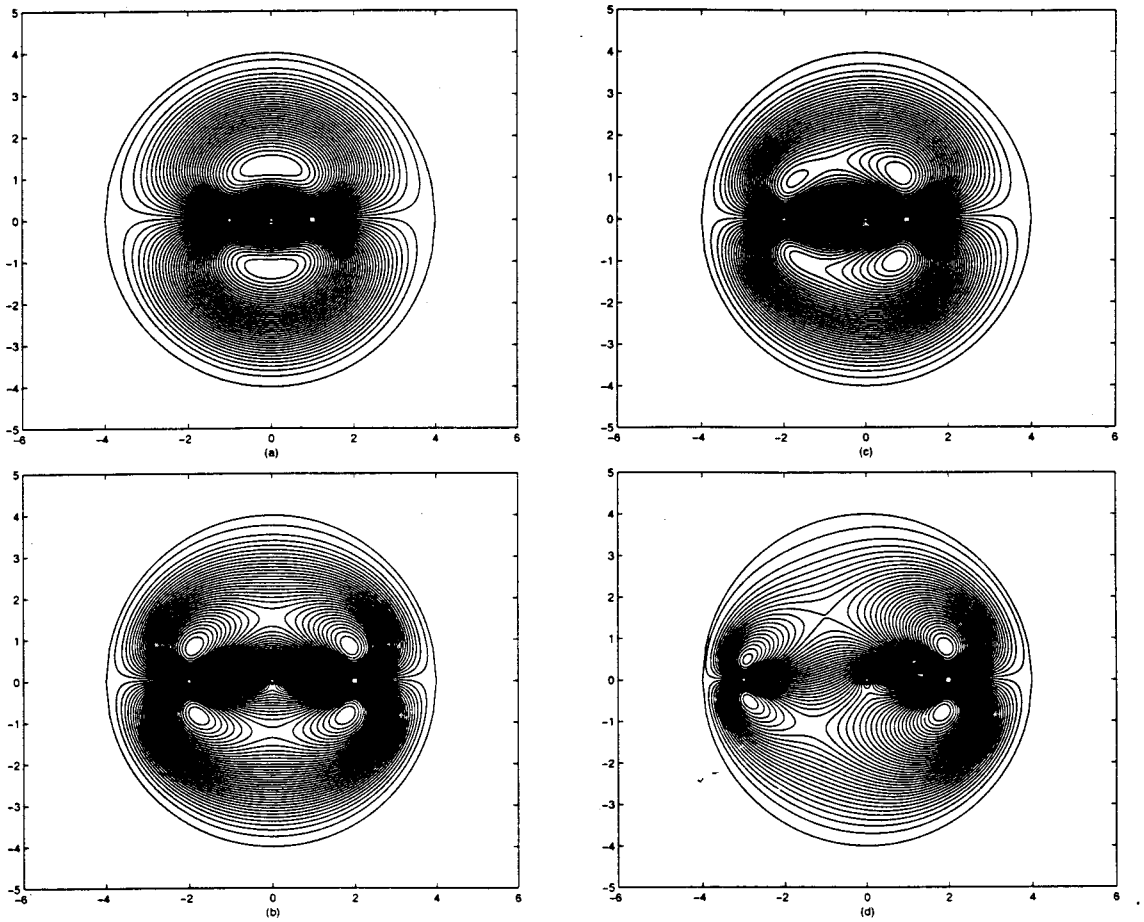

FIG. 13. Interior flows: Streamlines for a pair of equal stokeslets ($F=F'=1$) with their axes along the x-direction for various stokeslet locations. Here the rotation parameter is fixed at $k=0.1$. (a) $c=1.0$, $c'=1.0$; (b) $c=2.0$, $c'=2.0$; (c) $c=1.0$, $c'=2.0$; (d) $c=2.0$, $c'=3.0$.

may be obtained by putting $F'=0$ in Eq. (23). It may be worthwhile to point out that this solution has not been derived before in the literature. Below, we use the solution in Eq. (23) to discuss the flow topologies for a pair of stokeslets.

The flow patterns for a pair of equal stokeslets with their axes parallel to the x-axis for several values of k are shown in Fig. 12. Here, the equidistant stokeslets are located very close to the wall. For smaller values of k, different sets of eddies are generated in the flow region as shown in Fig. 12(a). In the upper half of the cylinder, a pair of symmetric eddies appears each in the neighborhood of the stokeslets. Right below these eddies, the streamlines between the stokeslets have nonuniform curvature, yielding an attached eddy which is symmetrical about the y-axis. In the lower half of the cylinder, the structure of the flow topologies is qualitatively the same as those in the upper half but quantitatively different. A pair of symmetric eddies appears each in the neighborhood of the stokeslets but with their sizes smaller than those in the upper half. Right below these eddies, the fluid migrates between the stokeslets as it does in the upper half, but with nearly uniform curvature. At the center the flow is circulatory as expected. It is interesting that the streamlines due to the migration of the fluid in the two regions cross each other, giving birth to a pair of stagnation points in the lower half of the cylinder [not shown in Fig. 12(a)]. The flow structure described above continues for all smaller values of the rotation parameter k as seen from Figs. 12(b)–12(c). The locations of the stagnation points are displayed in these plots. It is also clear from these plots that the structure of the different eddies changes as we increase k. Indeed, the symmetric eddies (in the upper as well as in the lower half) shrink while the attached eddy (in the upper half) grows as we gradually increase the value of k. We also notice that the circulatory flow region around the center grows. The symmetric eddies continue to shrink as we increase the value of k as shown in Figs. 12(d)–12(e). When $k=0.8$, the symmetric eddies in the lower half disappears while the size of those in the upper half become smaller [see Fig. 12(f)]. It may be worthwhile to point out that for higher values of k, the fluid migration increases and the circulatory flow around the center becomes intense.

In Fig. 13, the flow topologies due to a pair of equal stokeslets are shown for various stokeslet locations with fixed $k=0.1$. When the stokeslets are close to the center located at $c=c'=1$, two attached eddies in each half symmetrical about the x-axis appear as shown in Fig. 13(a). If we move the stokeslets away from the center ($c=c'=2$), a pair of smaller eddies are generated within each attached eddy as seen from Fig. 13(b). The streamline crossing seems to occur

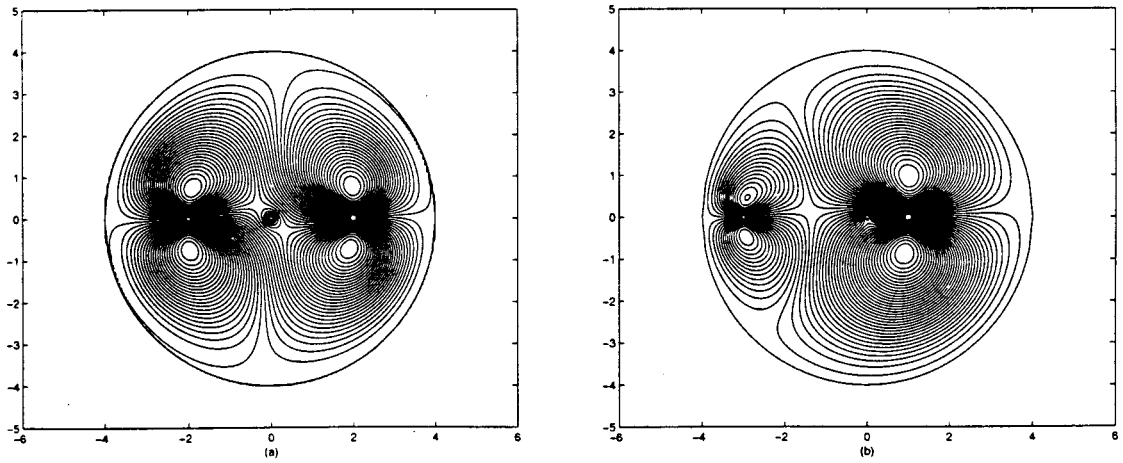

FIG. 14. Interior flows: Streamlines for a pair of opposite stokeslets ($F=-F'=1$) with their axes along the x-direction for several stokeslet locations. Here the rotation parameter is fixed at $k=0.1$. (a) $c=2.0$, $c'=2.0$; (b) $c=1.0$, $c'=3.0$.

at the y-axis and so one would expect a pair of stagnation points on this axis. The circulatory flow around the center increases as we move the stokeslets away from it. The flow structures for nonequidistant stokeslets are illustrated in Figs. 13(c)–13(d). The flow in this case is symmetrical about the x-axis but not about the y-axis.

The flow patterns for a pair of opposite stokeslets for two different locations are shown in Fig. 14. For a fixed value of $k=0.1$, the flow has quantitatively different features for the two stokeslets positions as seen from Figs. 14(a)–14(b). If the stokeslets are equidistant, a larger eddy with two cores and enclosing the center appear as in Fig. 14(a). This eddy has the shape of a figure eight. An interior streamline of this eddy appears to collide with a circular streamline of the circulatory flow region around center indicating the birth of a pair of stagnation points. Right outside the figure eight shaped eddy, a pair of symmetric eddies appears at diagonally opposite flow regimes. In the case of nonequidistant stokeslets, the figure eight shaped eddy occurs away from the center. Here it appears that there is a single stagnation point in the flow which possibly occurs on the x-axis. This stagnation point appears to be the center of a double homoclinic orbit. The eddies at the diagonally opposite regimes are smaller in the present case.

C. Pair of stokeslets with their axes along the *y*-direction

We consider a pair of stokeslets of strengths F and F' positioned at $(r,\theta)=(c,0)$, and $(r,\theta)=(c',\pi)$, respectively. Here $c,c'>a$. The axes of these stokeslets are taken to be along the y-direction. The stream function corresponding to this pair of stokeslets in an unbounded flow is given in Eq. (17). The complete solution in the presence of a cylinder is

$$\psi(r,\theta)=F\left[-(r\cos\theta-c)\log R+\left(r\cos\theta-\frac{a^2}{c}\right)\log\frac{cR_1}{a}+\frac{(c^2-a^2)\left(\frac{r^2}{a^2}-1\right)}{2c}\,\frac{r\left(r-\frac{a^2}{c}\cos\theta\right)}{R_1^2}-\frac{(c^2-a^2)}{c}\log\frac{cR_1}{a}\right]$$
$$+F'\left[(r\cos\theta+c')\log R'-\left(r\cos\theta+\frac{a^2}{c'}\right)\log\frac{c'R_1'}{a}+\frac{(c'^2-a^2)\left(\frac{r^2}{a^2}-1\right)}{2c'}\,\frac{r\left(r+\frac{a^2}{c'}\cos\theta\right)}{R_1'^2}-\frac{(c'^2-a^2)}{c'}\log\frac{c'R_1'}{a}\right]. \tag{24}$$

The solution for a single stokeslet located inside a cylinder may be deduced from Eq. (24) by taking $F'=0$ and this solution does not seem to have been obtained before. Next we use the solution in Eq. (24) to discuss the flow topologies in the case of a pair of stokeslets along the y-direction.

The flow topologies for a pair of equal stokeslets with their axes parallel to the y-direction for various values of k are displayed in Fig. 15. Here, the stokeslets are located equidistant from the center ($c=c'=1.0$). A symmetric pair of attached eddies occur adjacent to each stokeslet. The fluid exhibits a rotational flow surrounding the origin in the region between these two eddies [see Figs. 15(a)–15(b)]. For the values of $k>0.5$, two symmetric pairs of smaller eddies are generated in the vicinity of the origin in addition to the al-

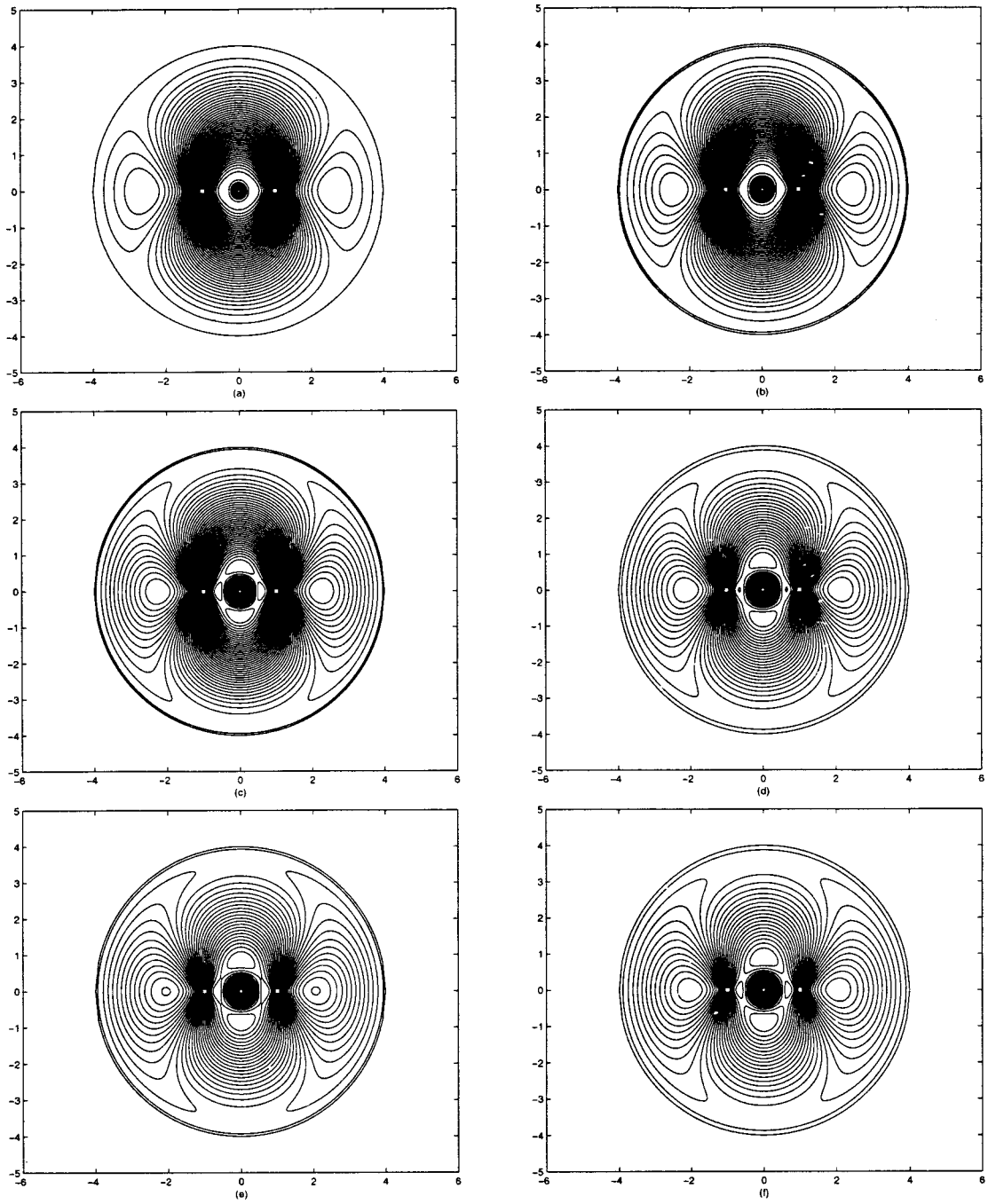

FIG. 15. Interior flows: Streamlines for a pair of equal ($F=F'=1$) and equidistant ($c=c'=1.0$) stokeslets with their axes along the y-direction for various values of the rotation parameter k. (a) $k=0.3$; (b) $k=0.5$; (c) $k=0.7$; (d) $k=0.85$; (e) $k=0.9$; (f) $k=0.95$.

ready existing eddies as seen from Figs. 15(c)–15(f). Furthermore, the streamline crossing occurs near the center yielding four stagnation points. These interior saddle points are seen more clearly in Fig. 15(e).

In Fig. 16, the flow patterns for a pair of equal stokeslets for various stokeslets locations with fixed $k=0.9$ are shown. When the stokeslets are equidistant from the center, several eddy patterns are seen in the flow field. For the values of $c=c'=2$, three concentric circulatory flow regions are seen in the flow field. The first circulatory region appears in the vicinity of the center and is trapped between a pair of symmetric eddies. The second region occurs engulfing the first circulatory region, the pair of eddies, and the stokeslets. Just outside this second circulatory region, another pair of symmetric eddies are generated as shown in Fig. 16(a). Finally, the third circulatory region is seen adjacent to the wall. If the stokeslets are moved further away from the center ($c=c'=3$), the flow again has three circulatory regions but the size of those symmetric eddies change considerably [see Fig. 16(b)]. The symmetric pair of eddies adjacent to the first circulatory region grow in size while the pair adjacent to the second region shrinks. The above flow structure prevails even in the case of nonequidistant stokeslet positions. However, in the latter case the sizes of the eddies change due to

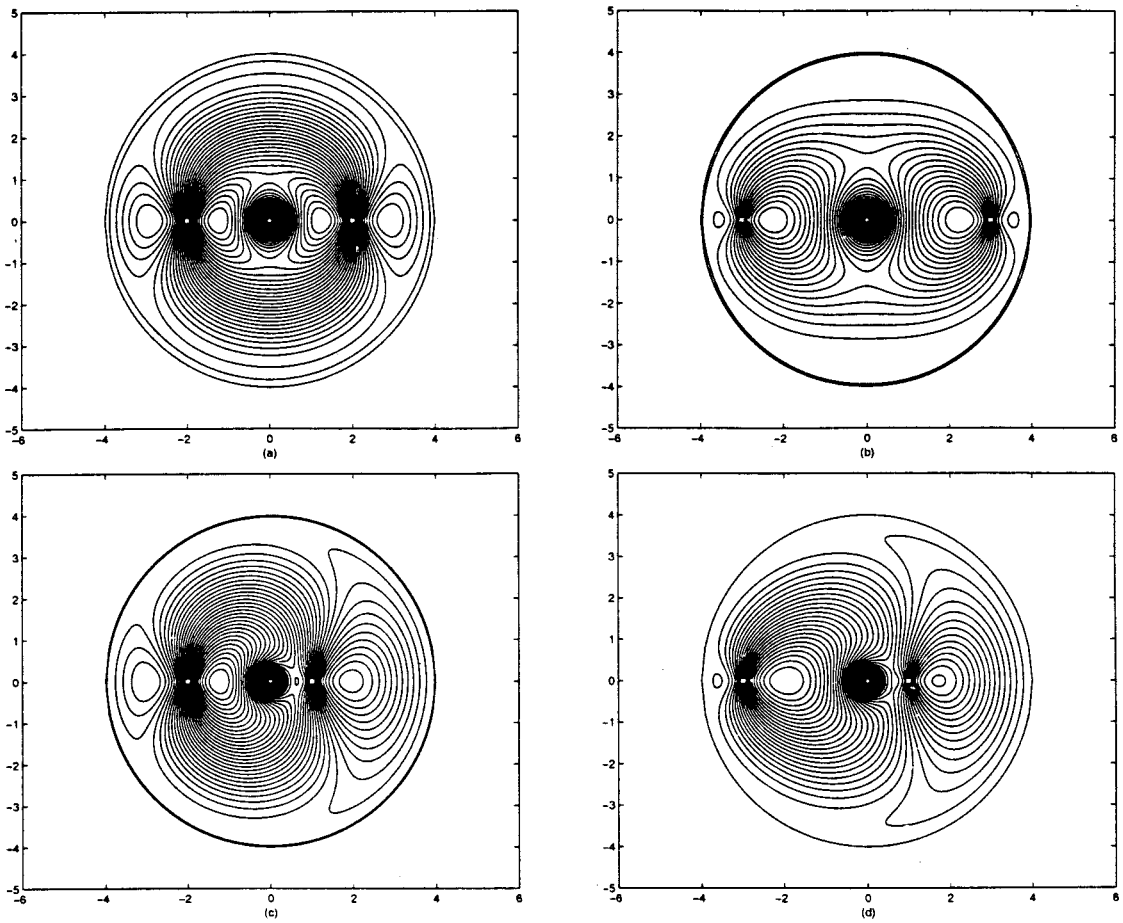

FIG. 16. Interior flows: Streamlines for a pair of equal stokeslets ($F=F'=1$) with their axes along the y-direction for various stokeslet locations. Here the rotation parameter is fixed at $k=0.9$. (a) $c=c'=2.0$; (b) $c=c'=3.0$; (c) $c=1.0$, $c'=2.0$; (d) $c=1.0$, $c'=3.0$.

eccentric locations of the stokeslets. The eddy that appears next to the stokeslet closer to the center is bigger and the one that exists next to the stokeslet away from the center is smaller. These features are shown in Figs. 16(c)–16(d).

The streamline patterns for a pair of opposite stokeslets for two different locations with fixed $k=0.9$ are shown in Fig. 17. If the stokeslets are equidistant ($c=c'=1$), an attached larger eddy enclosing the stokeslets and the center appears as depicted in Fig. 17(a). Just outside this, another attached eddy smaller in size exists. Of course, the flow is circulatory around the center. If the stokeslets are at nonequidistant positions ($c=1.0, c'=2.0$), the larger eddy grows and the smaller eddy shrinks as shown in Fig. 17(b). The streamlines due to the stokeslet closer to the origin and the circular streamlines around the origin intersect yielding a pair of stagnation points in the flow. These two saddle points appear on the positive side of the x-axis.

V. CONCLUSION

Singularity induced two-dimensional Stokes flows inside and outside a circular cylinder are studied by careful investigation of the level sets of stream functions of these flows. The types of singularities considered here include rotlets and stokeslets. The exact expression for the stream function for each of these flows is obtained by using the straightforward Fourier expansion method. In all of these flows, the axes of the line singularities are assumed to be parallel to the axis of the cylinder and all of these axes lie in one plane. In the plane of flow, the x-axis contains all of these singularities and the center of the cylinder.

The first part of this paper investigates flows past a cylinder for various combinations (strengths and locations) of the singularities. The far-field behavior in all of these cases is that of uniform flow with speed and flow direction depending on the primary singularities and their locations. In the case of a pair of rotlets and a pair of stokeslets with their axes along the y-direction, the far-field uniform flow vanishes if the primary singularities have equal strengths. In the case of a pair of stokeslets along the x-direction, the uniform flow vanishes if the primary stokeslets have opposite strengths. The streamlines are plotted in each case in order to display interesting flow patterns and eddies of different shapes, sizes, and structures. In the presence of rotation of the cylinder, eddies of unusual sizes and shapes appear in the case of a pair of rotlets. The rotation parameter also significantly influences the eddy structure in the case of a pair of stokeslets.

The second part discusses the flows inside the cylinder in the presence of same singularity types as above. Eddies of different sizes and shapes occur and their structures depend on the rotlet locations. In the presence of the cylinder rota-

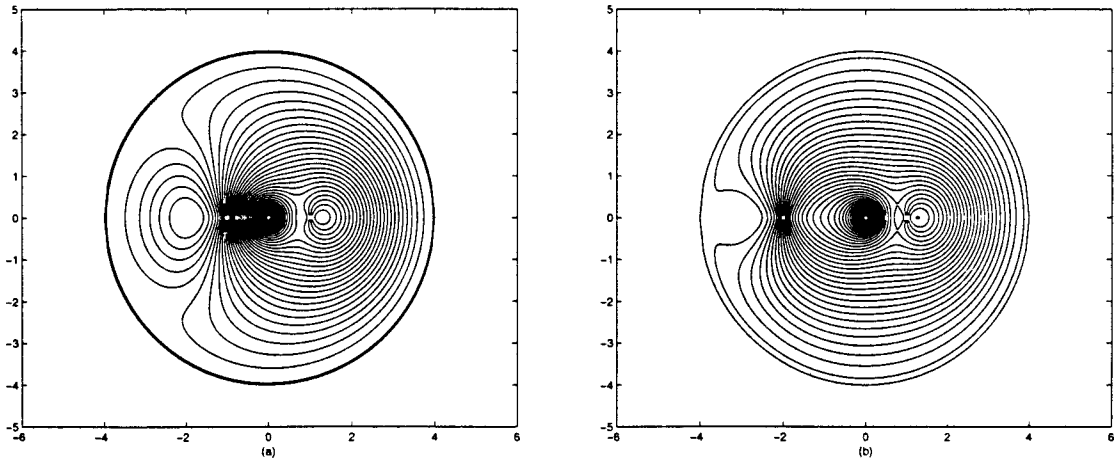

FIG. 17. Interior flows: Streamlines for a pair of opposite stokeslets ($F=-F'=1$) with their axes along the y-direction for several rotlet locations. Here the rotation parameter is fixed at $k=0.9$. (a) $c=c'=1.0$; (b) $c=1.0$, $c'=2.0$.

tion, the flow structure changes significantly and the streamline plots reveal the existence of homoclinic and heteroclinic orbits. Forcing time dependence in these flows in an appropriate manner so to alternate between these steady Stokes flows with different homoclinic and heteroclinic orbits may generate interesting Lagrangian chaotic flows.

ACKNOWLEDGMENT

This research has been partially supported by the interdisciplinary research program of the Office of the Vice President for Research and Associate Provost for Graduate Studies under Grant No. IRI-98.

[1]G. G. Stokes, ''On the effect of internal friction of fluids on the motion of pendulums,'' Trans. Cambridge Philos. Soc. **9**, 8 (1851) [see also Scientific Papers **3**, 141 (1901)].
[2]H. Lamb, *Hydrodynamics* (Dover, New York, 1932).
[3]J. Happel and H. Brenner, *Low Reynolds Number Hydrodynamics* (Martinus Nijhoff, The Hague, 1983).
[4]S. Kim and S. J. Karrila, *Microhydrodynamics: Principles and Selected Applications* (Butterworth-Heinemann, Boston, 1991).
[5]C. Pozrikidis, *Boundary Integral and Singularity Methods for Linearized Viscous Flow* (Cambridge University Press, Cambridge, MA, 1992).
[6]G. K. Batchelor, ''The stress system in a suspension of force-free particles,'' J. Fluid Mech. **41**, 545 (1970).
[7]H. A. Lorentz, ''A general theorem concerning the motion of a viscous fluid and a few consequences derived from it,'' Verst. Kon. Akad. Wet. Ams. **5**, 168 (1897).
[8]C. W. Oseen, ''Uber die Stokessche Formel und eine verwandt Aufgabe inder Hydrodynamik,'' Ark. Mat., Astron. Fys. **6**, 29 (1910).
[9]J. M. Burgers, ''On the motion of small particles of elongated form suspended in a viscous fluid,'' Kon. Ned. Akad. Wet. **16**, 113 (1938).
[10]J. R. Blake, ''A note on the image system for a stokeslet in a no-slip boundary,'' Proc. Cambridge Philos. Soc. **70**, 303 (1971).
[11]J. R. Blake and A. T. Chwang, ''Fundamental singularities of viscous flow. Part I. The image systems in the vicinity of a stationary no-slip boundary,'' J. Eng. Math. **8**, 23 (1974).
[12]S. Kaplun and P. A. Lagerstorm, ''Asymptotic expansion of Navier–Stokes solution for small Reynolds numbers,'' J. Math. Mech. **6**, 585 (1957).
[13]I. Proudman and J. R. A. Pearson, ''Expansions at small Reynolds numbers for the flow past a sphere and a circular cylinder,'' J. Fluid Mech. **2**, 237 (1957).
[14]G. B. Jeffery, ''The rotation of two circular cylinders in a viscous fluid,'' Proc. R. Soc. London, Ser. A **101**, 169 (1922).
[15]J. M. Dorrepaal, M. E. O'Neill, and K. B. Ranger, ''Two-dimensional Stokes flows with cylinders and line singularities,'' Mathematika **31**, 65 (1984).
[16]W. W. Hackborn, ''On a class of Stokes flows inside a corrugated boundary,'' Q. Appl. Math. **L1**, 329 (1993).
[17]S. H. Smith, ''Some limitations of two-dimensional unbounded Stokes flow,'' Phys. Fluids A **2**, 1724 (1990).
[18]A. Avudainayagam and B. Jothiram, ''No-slip images of certain line singularities in a circular cylinder,'' Int. J. Eng. Sci. **25**, 1193 (1987).
[19]S. H. Smith, ''A note on Stokes flow due to a line rotlet,'' Mathematika **42**, 127 (1995).
[20]B. Y. Ballal and R. S. Rivlin, ''Flow of a Newtonian fluid between eccentric rotating cylinders: Inertial effects,'' Arch. Ration. Mech. Anal. **62**, 237 (1976).
[21]S. C. Jana, G. Metcalfe, and J. M. Ottino, ''Experimental and computational studies of mixing in complex Stokes flows: The vortex mixing flow and multicellular cavity flows,'' J. Fluid Mech. **269**, 199 (1994).
[22]H. Power, ''The completed double layer boundary integral equation method for two-dimensional Stokes flow,'' IMA J. Appl. Math. **51**, 123 (1993).
[23]S. H. Smith, ''The Jeffery paradox as the limit of three-dimensional Stokes flow,'' Phys. Fluids A **2**, 661 (1990).
[24]K. B. Ranger, ''Eddies in two-dimensional Stokes flow,'' Int. J. Eng. Sci. **18**, 181 (1980).
[25]N. Liron and J. R. Blake, ''Existence of viscous eddies near boundaries,'' J. Fluid Mech. **107**, 109 (1981).
[26]J. R. Blake and S. R. Otto, ''Ciliary propulsion, chaotic filtration and a 'blinking stokeslet','' J. Eng. Math. **30**, 151 (1996).
[27]V. V. Meleshko and H. Aref, ''A blinking rotlet model for chaotic advection,'' Phys. Fluids A **8**, 3215 (1996).